NASA TN D-393

TECHNICAL NOTE
D-393

MEASUREMENTS OF THE TIME-AVERAGED AND INSTANTANEOUS INDUCED VELOCITIES IN THE WAKE OF A HELICOPTER ROTOR HOVERING AT HIGH TIP SPEEDS

By Harry H. Heyson

Langley Research Center
Langley Field, Va.

NATIONAL AERONAUTICS AND SPACE ADMINISTRATION
WASHINGTON
July 1960

M

NATIONAL AERONAUTICS AND SPACE ADMINISTRATION

TECHNICAL NOTE D-393

MEASUREMENTS OF THE TIME-AVERAGED AND INSTANTANEOUS INDUCED VELOCITIES IN THE WAKE OF A HELICOPTER ROTOR HOVERING AT HIGH TIP SPEEDS

By Harry H. Heyson

SUMMARY

Measurements of the time-averaged induced velocities were obtained for rotor tip speeds as great as 1,100 feet per second (tip Mach number of 0.98) and measurements of the instantaneous induced velocities were obtained for rotor tip speeds as great as 900 feet per second. The results indicate that the small effects on the wake with increasing Mach number are primarily due to the changes in rotor-load distribution resulting from changes in Mach number rather than to compressibility effects on the wake itself. No effect of tip Mach number on the instantaneous velocities was observed. Under conditions for which the blade tip was operated at negative pitch angles, an erratic circulatory flow was observed.

INTRODUCTION

One possible means of increasing the forward speed and the lifting capacity of a helicopter rotor is to increase the rotor tip speed. The degree to which the tip speed can be increased is limited, however, by compressibility losses, increased noise levels, and the large fuselage down loads which accompany the increased downwash velocities. In order to evaluate these factors, several 10-foot-diameter rotors have been tested in static thrust, and tip Mach numbers as high as 1 have been obtained. The performance and noise measurements obtained during these tests have been presented in references 1 and 2.

During the more recent tests, rakes of total-head and static-pressure tubes were used to study the time-averaged induced-velocity distribution in the rotor wake. These measurements were obtained throughout almost the entire range of the tests; that is, for disk loadings from 0 to 21.5 pounds per square foot and for tip speeds from 500 feet per second to 1,100 feet per second. These data are presented herein and studied to indicate the trend of the effect of tip speed (and thus Mach number) on the induced-velocity distribution in the wake.

A few measurements of the instantaneous induced velocities in the wake were obtained by means of a single hot-wire anemometer at one location below the rotor. This instrument was used to obtain the root-mean-square value of the fluctuating components of induced velocity at tip speeds as high as 900 feet per second. For a few conditions, the time-history shape of the induced-velocity pulses was also obtained.

SYMBOLS

C_T rotor thrust coefficient, $\frac{\text{Thrust}}{\rho\pi R^2(\Omega R)^2}$

R rotor radius, ft

r radial distance from rotor axis, ft

t time, sec

w local induced velocity, positive upward, fps

$\overline{w}$ root-mean-square value of fluctuating components of local induced velocity, fps

w_0 momentum-theory value of induced velocity, positive upward, $-\Omega R\sqrt{\frac{C_T}{2}}$, fps

z vertical distance from rotor, positive upward, ft

$\theta_{.75}$ blade pitch angle at 0.75 blade radius, deg

ρ mass density of air, slugs/cu ft

Ω rotor rotational speed, radians/sec

EQUIPMENT AND TESTS

The 10-foot-diameter rotor employed in these tests had two blades mounted in a teetering or "see-saw" hub. Each blade (fig. 1(a)) had 2:1 plan-form taper, linear washout of 12°, and NACA 0012 airfoil sections. The rotor was tested on a whirlstand mounted in the Langley full-scale tunnel (fig. 1(b)). The rotor was mounted approximately

1.5 diameters above the wind-tunnel floor. The lips of the entrance cone, the nearest obstruction, were approximately 3 diameters from the rotor tips. The use of this wind tunnel provided both an available balance for thrust measurement and a large enclosed space free of extraneous wind effects.

Time-averaged induced velocities were measured by rakes of total-head and static-pressure tubes at two vertical distances ($z/R = -0.145$ and $z/R = -0.450$) below the rotor. At each location, two rakes were provided; one with the tubes pointed upward in order to measure downwash velocities, and the other with the tubes pointed downward in order to measure upwash velocities. One pair of tubes was located at each of the following radial positions r/R:

L
8
3
6

Downwash rakes		Upwash rakes	
0.20	0.70	0.20	0.82
.24	.74	.24	.86
.28	.77	.28	.90
.32	.79	.32	.94
.36	.83	.36	.98
.40	.87	.50	1.08
.47	.91	.73	1.18
.57	.95	.78	
.62	1.05		
.66	1.15		

The damping inherent in the combination of pressure tubes, manometer, and connecting tubing is sufficiently great to allow the assumption that the manometer readings will represent the time-averaged pressures.

A constant-temperature hot-wire anemometer was installed at one position ($z/R = -0.145$, $r/R = 0.67$) in order to measure the instantaneous induced velocities. (See fig. 1(c).) The hot-wire anemometer and its associated circuits are the same as those described in reference 3. The circuits were arranged so that the root-mean-square value of the fluctuating components of velocity could be obtained. In addition, the waveform could be displayed on the face of an oscilloscope and photographed.

The hot wire itself was mounted so that, when the blade was directly above the wire, the length of the wire was parallel to the blade axis. Since a hot wire senses only those velocities normal to its length, the hot wire was insensitive to radial velocities during these tests. With the equipment used, which removes the average velocity from the hot-wire output, the hot wire, as usual, will measure essentially only the

fluctuations of velocity in the direction of the main flow, provided that the main flow has a reasonably high velocity. If, however, the average velocity of the main flow is zero, the hot wire measures the fluctuations of the resultant of the horizontal and vertical velocities. At low speeds other than zero the hot wire will provide an unequally weighted average fluctuation. These effects are all inherent in the data to be presented since no corrections have been applied.

The tests were conducted by running the rotor at specified tip speeds with the blade pitch locked. During the course of the tests the temperature was not constant and, consequently, the Mach number corresponding to a given tip speed varied slightly. The data in this paper are presented in terms of tip speed. The approximate Mach number to which the tip speed corresponds may be obtained by dividing the tip speed by 1,115.

RESULTS AND DISCUSSION

Time-Averaged Induced Velocities

Velocities at edge of wake.- As noted previously, upwash and downwash velocities were measured on separate survey rakes with suitably oriented tubes. At certain points in the flow, notably near the edge of the wake, it was found that the two rakes simultaneously provided two entirely different values of induced velocity; one an upwash, the other a downwash. (See, for example, fig. 2.)

The ambiguity of the measured velocities may be explained by considering the characteristics of the pressure tubes in this flow, which fluctuates back and forth through zero velocity as the individual tip vortices pass along the edge of the wake. Each total-head tube senses the true total head only so long as it is pointed nearly directly toward the oncoming flow. When the flow is directed backward over the tube the pressure reading is small and spurious. Thus, in combination with the low response rate of the manometer, the upward-pointed tubes read an average of the flow for that portion of time during which the flow is directed downward, and, similarly, the downward-pointed tubes read an average only of the upward velocities. Unfortunately, the tubes are quite inaccurate in the presence of the relatively large sidewash velocities which may exist as the wake vortices pass the tube. Thus, the survey measurements near the edge of the wake cannot simply be averaged to find the correct induced velocity.

In the present paper, the induced-velocity data near the wake edge have been faired in the manner shown in figure 2. All readings which definitely indicated a flow in the incorrect direction for a particular

tube orientation have been eliminated. In view of the foregoing considerations, all faired data for locations at and outside the wake edge should be considered as indicating only the order of magnitude of the average velocities in this region.

Effect of blade pitch angle.- Figures 3 and 4 present the nondimensional induced-velocity distribution in the rotor wake for various blade pitch angles. The trends shown are the same regardless of tip speed or vertical position in the wake. At the lowest pitch angle of 2°, the wake is somewhat narrower in diameter than at the other pitch angles, corresponding to the fact that for this case the blade tip is at a negative local pitch angle. At pitch angles of the order of 4° or 5°, the wake is essentially uniform with a very sharp increase at the wake edges. At higher pitch angles the wake becomes increasingly nonuniform with the peak induced velocities near the outer edge of the wake.

The character of the wake, as described above, is essentially that which would be indicated on the basis of the expected load distribution for these twisted and tapered blades. (See figs. 5 and 6.)

Wake at near-zero lift.- The measured data for zero pitch (fig. 7) are worthy of some attention because of the implications for performance calculations when portions of the blade are at large positive pitch angles while others may be at significant negative pitch angles. In the present case, when the pitch at the 0.75-radius point is zero, the local pitch at the blade tip is -3° and at the inboard cutout the blade pitch is about 7°. Thus, simple blade-element theory would predict downwash velocities at the inboard end of the blades and an upwash velocity at the blade tips. As shown by figure 7 this does not appear to be the case. Even though the measurement accuracy is very poor at these low velocities, it would appear that there is a mild upwash below the entire rotor. (Notice that the rotor lift is negative for this condition. For a rotor with positive lift, the measurements would correspond to a downwash above the entire rotor.)

It is evident that there must be large-scale distortions of the flow from that assumed in the theory, and that in consequence of these distortions, the ability of theory to predict the performance accurately under these conditions is questionable. Fortunately, in this case, the forces involved are so small that the errors in performance are of small magnitude. This, however, is not always true, as larger errors could be introduced in the case, for example, of the static-thrust performance of a very highly twisted propeller. This flow field at low lift will be discussed further in a subsequent section of this paper.

Effect of tip Mach number.- Figures 8 and 9 show the effect of tip Mach number (tip speed) on the distribution of induced velocity in the rotor wake. The data indicate, in general, only small changes in the

nondimensional induced velocity with Mach number. These changes are usually confined to locations near the outer portion of the wake where the induced-velocity ratio, in general, shows a small increase. The increase in induced velocity is, of course, caused by the effect of Mach number on the lifting effectiveness of the outer part of the blades. This increased effectiveness, in turn, alters the rotor-disk-load distribution. Thus it is the effect of Mach number on the disk-load distribution, rather than any direct compressibility effect on the wake itself, which alters the induced-velocity distribution in the wake.

Instantaneous Induced Velocities

Root-mean-square velocity fluctuations.- Figures 10 and 11 present the results of the hot-wire anemometer measurements. It is immediately evident that for the range of variables covered, tip Mach number has a negligible effect on the root-mean-square value of the velocity pulses. The root-mean-square velocity fluctuation remains between 7 and 14 percent of the local induced velocity for all but the lowest blade pitch angles. (See fig. 10.) Even this small fluctuation in velocity is several times that which can be credited to the bound vortices on the blades. Rough calculations, with the wake assumed to be in the shape of a spiral vortex, indicate that the strong vortices leaving the blade tips probably account for approximately two-thirds of the velocity fluctuation at this position. The entire procedure is, however, too crude in hovering (ref. 4) to elaborate on.

Shape of velocity pulses.- A qualitative time history of the induced velocity in the wake was obtained by displaying the output of the hot-wire anemometer on an oscilloscope which was photographed with a special camera. As shown in figures 12 and 13, the shape of the time history of the induced-velocity ratio was essentially unaffected, except in period, by tip speed. These data further emphasize the fact that tip speed has essentially no effect by itself on the wake of the rotor.

Figure 14 shows the fluctuations in the velocities measured under the rotor at very low lift $\left(\theta_{.75} = 2^{\circ}\right)$. Although some periodic components can be seen in the velocity trace, the major indication of figure 14 is the randomness of the velocity fluctuations as compared with those of figures 12 and 13. Some indication of the magnitude of the observed fluctuations may be gained by noting that the induced-velocity scale of figure 14 has been compressed by a factor of 10 over the scales of figures 12 and 13. Attempts to obtain similar data at zero pitch angle did not succeed because the velocities were so erratic that the signal could not be kept on the face of the oscilloscope tube. This is further indication that the flow, when the blade tip is at negative lift, departs so widely from the theoretical concepts that blade-element-theory calculations are probably of little value.

CONCLUDING REMARKS

Data from a study of the induced velocities in the wake of a hovering rotor have been presented for tip speeds as great as 1,100 feet per second (tip Mach number of 0.98). Small changes in the wake were observed as the tip Mach number was increased. These changes were apparently due to the effect of Mach number on the load distribution rather than to any direct effect of compressibility upon the wake itself. Hot-wire measurements of the instantaneous velocities at one point in the wake, for tip speeds as great as 900 feet per second, are also given. These data indicate that Mach number had essentially no effect on either the root-mean-square velocity fluctuations or the wave shape of the velocity pulses in the wake.

At very low blade pitch angles, that is, at pitch angles for which the blade tip was operated at substantial negative lift, an erratic flow existed. The nature of this flow was such that the accuracy of blade-element theory under these conditions is doubtful.

Langley Research Center,
National Aeronautics and Space Administration,
Langley Field, Va., March 8, 1960.

REFERENCES

1. Jewel, Joseph W., Jr., and Harrington, Robert D.: Effect of Compressibility on the Hovering Performance of Two 10-Foot-Diameter Helicopter Rotors Tested in the Langley Full-Scale Tunnel. NACA RM L58B19, 1958.

2. Jewel, Joseph W., Jr.: Compressibility Effects on the Hovering Performance of a Two-Blade 10-Foot-Diameter Rotor Operating at Tip Mach Numbers Up to 0.98. NASA TN D-245, 1960.

3. Laurence, James C., and Landes, L. Gene: Auxiliary Equipment and Techniques for Adapting the Constant-Temperature Hot-Wire Anemometer to Specific Problems in Air-Flow Measurements. NACA TN 2843, 1952.

4. Heyson, Harry H.: An Evaluation of Linearized Vortex Theory as Applied to Single and Multiple Rotors Hovering In and Out of Ground Effect. NASA TN D-43, 1959.

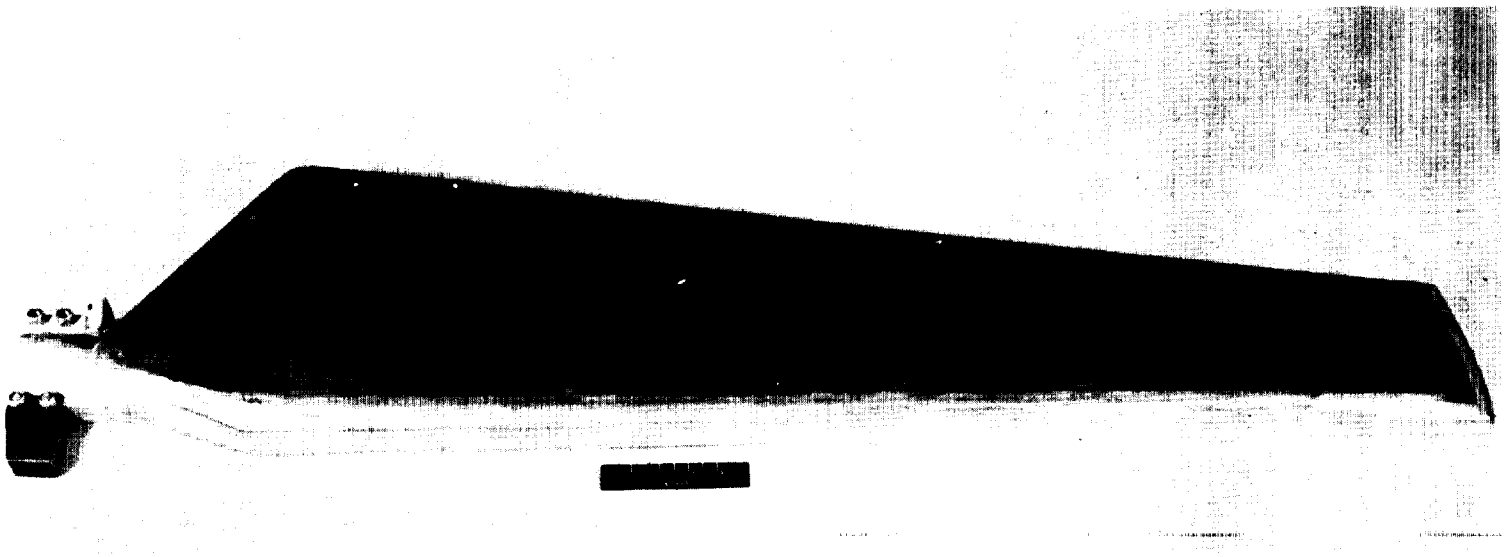

(a) Rotor blade. (Lower surface is shown.) L-58-868a

Figure 1.- Equipment used in tests.

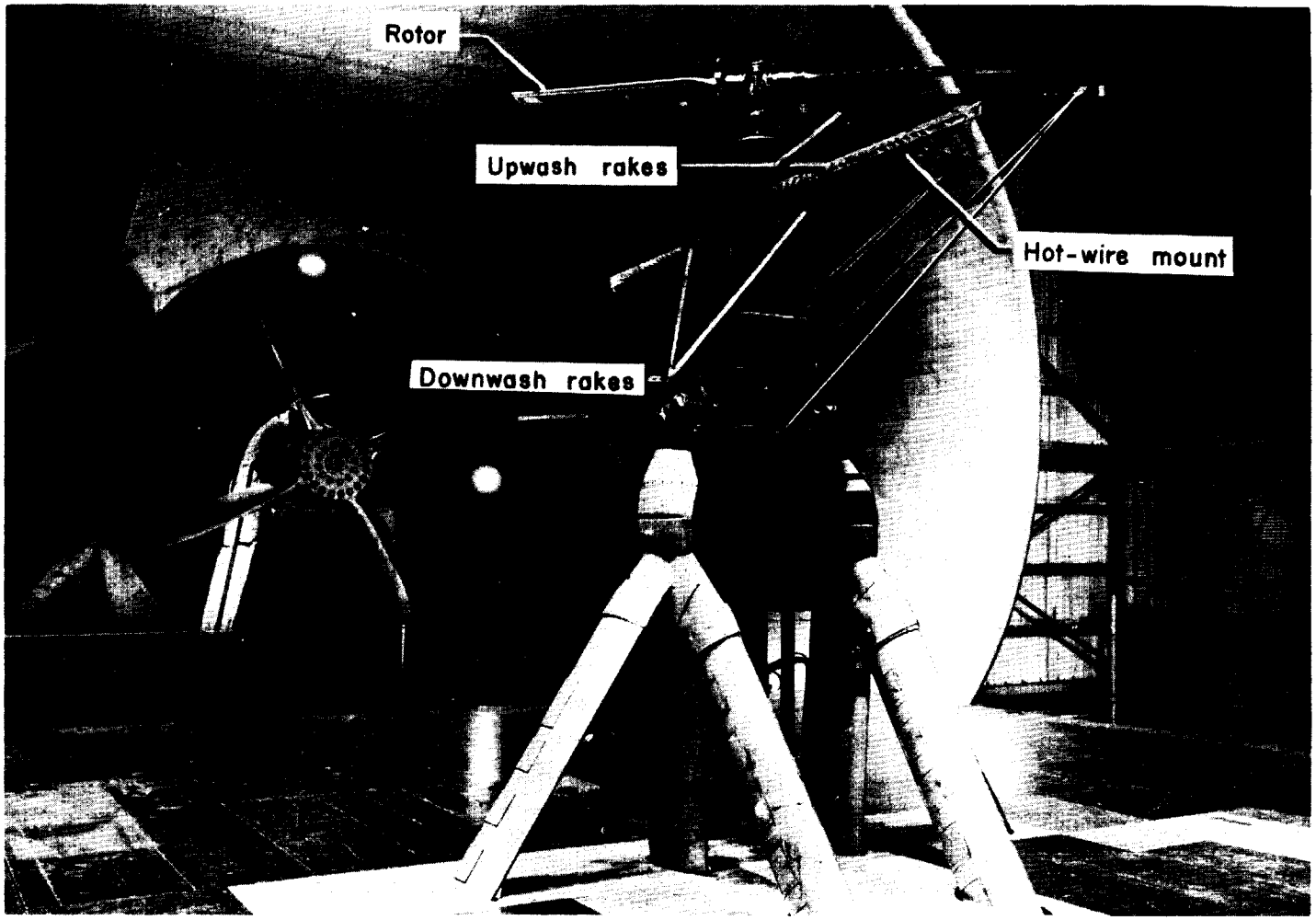

(b) General arrangement. L-58-1131a.1

Figure 1.- Continued.

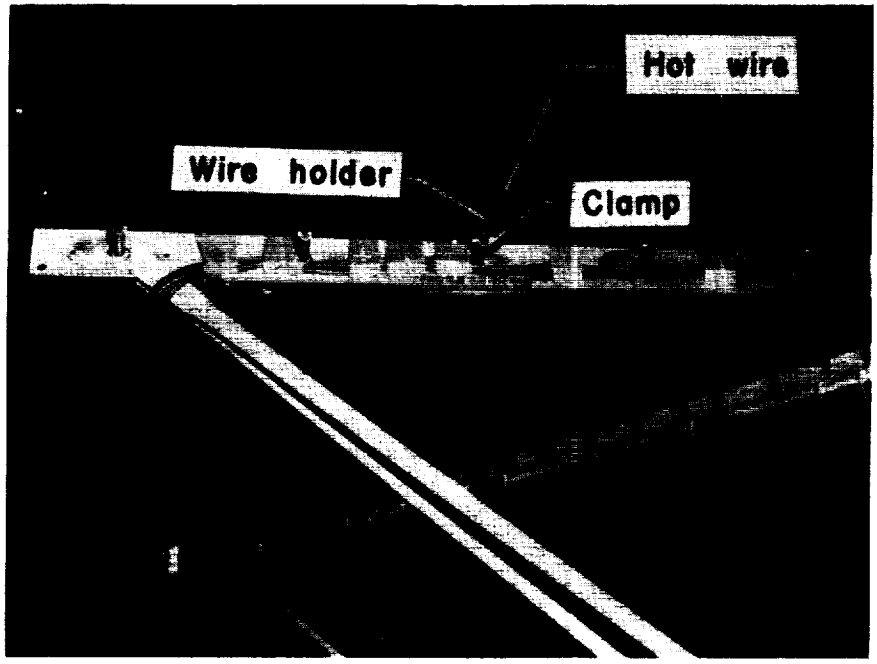

L-58-1139a.1

(c) Hot-wire anemometer and mount. (One upwash rake may be seen in background.)

Figure 1.- Concluded.

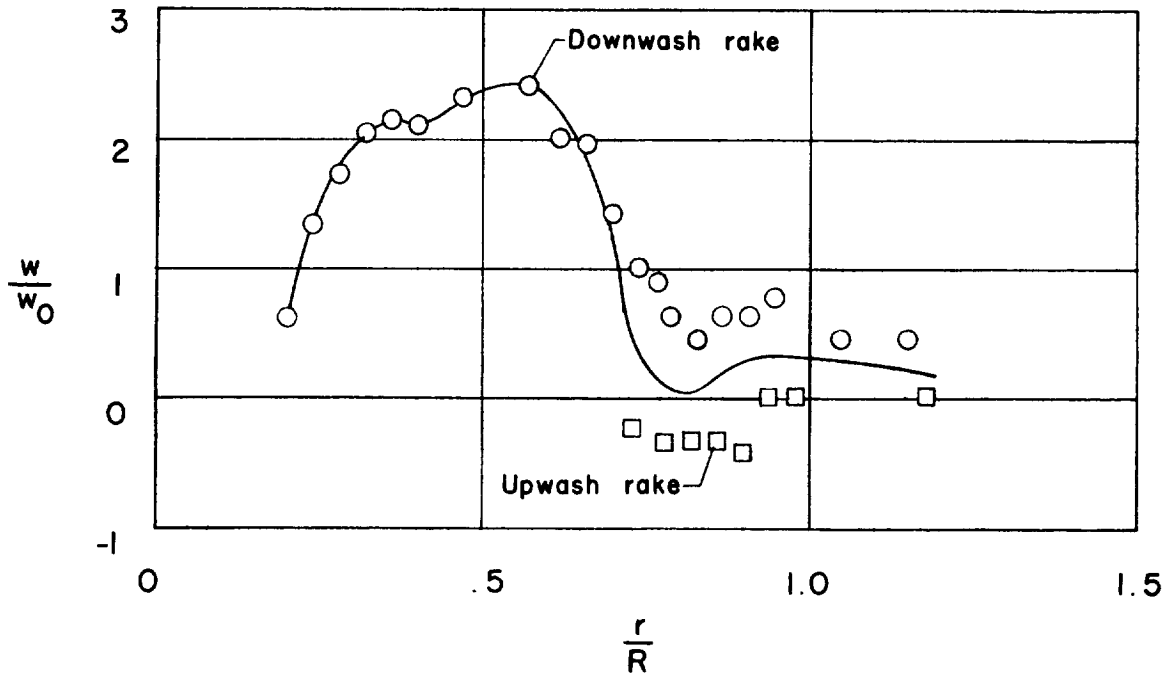

Figure 2.- Induced-velocity distribution below rotor at tip speed of 500 fps. $\theta_{.75} = 3^\circ$; $z/R = -0.145$.

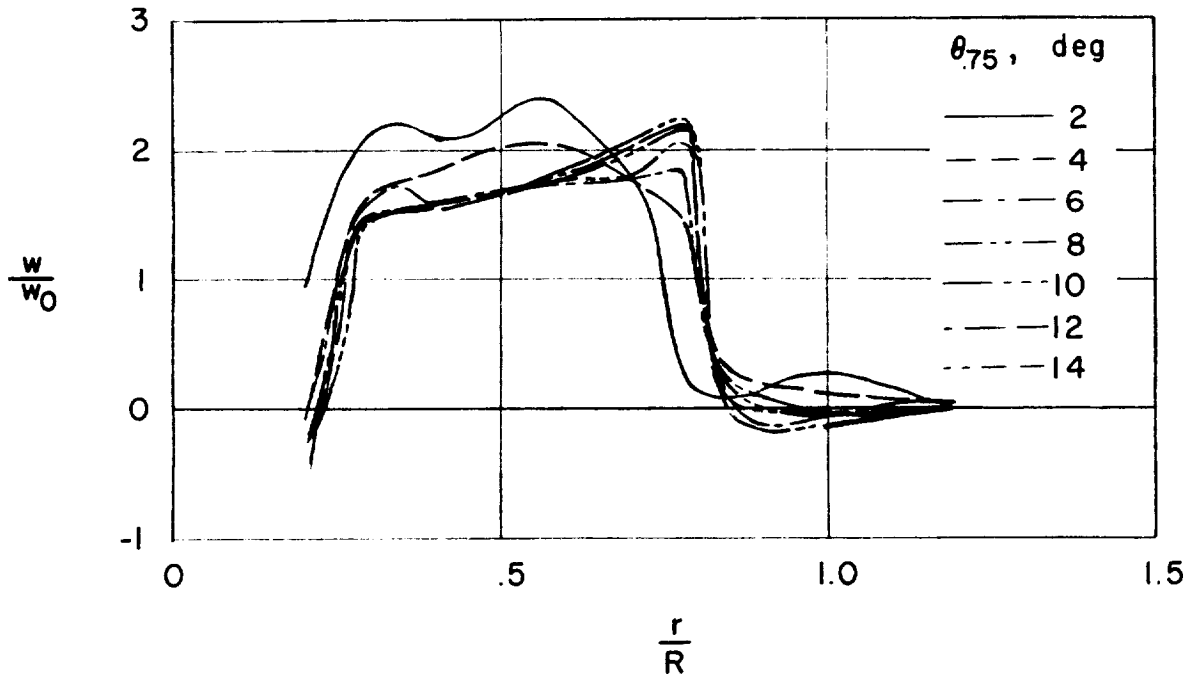

(a) ΩR = 500 fps.

Figure 3.- Effect of blade pitch angle at the 0.75R station on the induced velocities at z/R = -0.145.

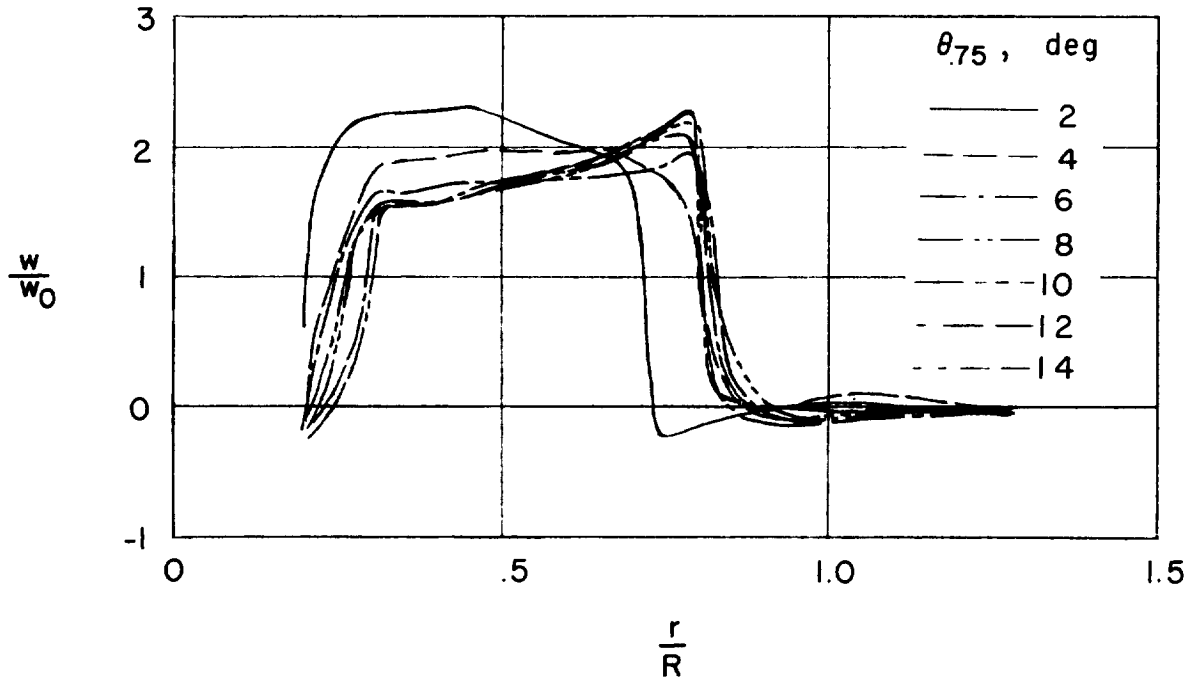

(b) ΩR = 700 fps.

Figure 3.- Continued.

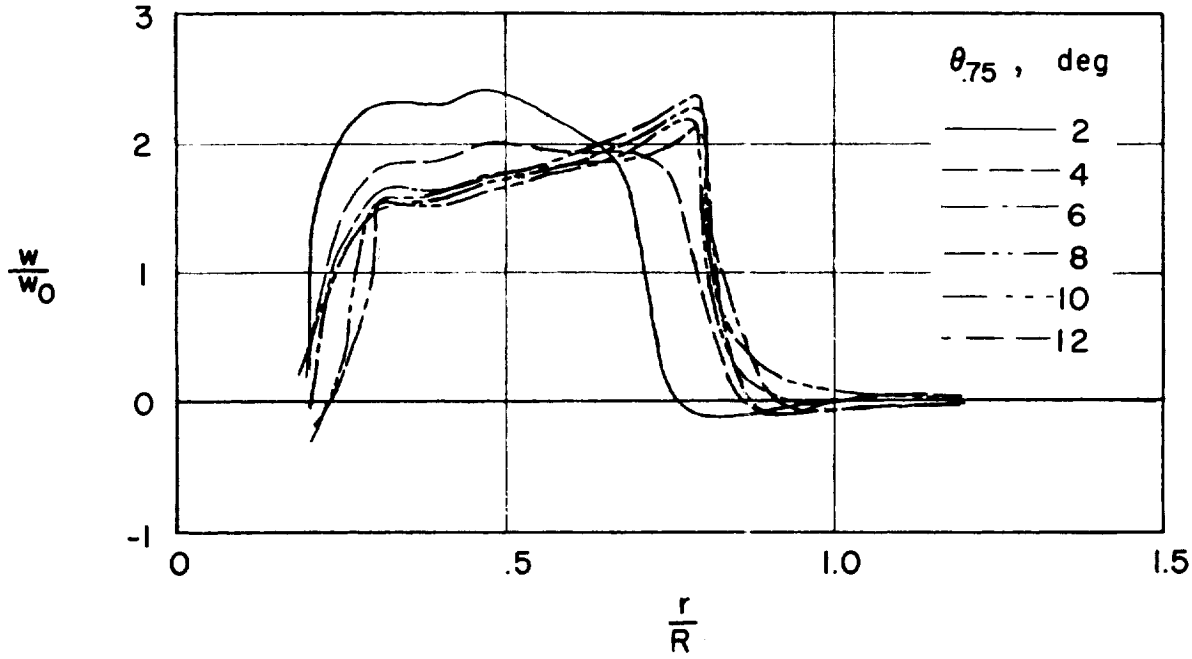

(c) ΩR = 900 fps.

Figure 3.- Continued.

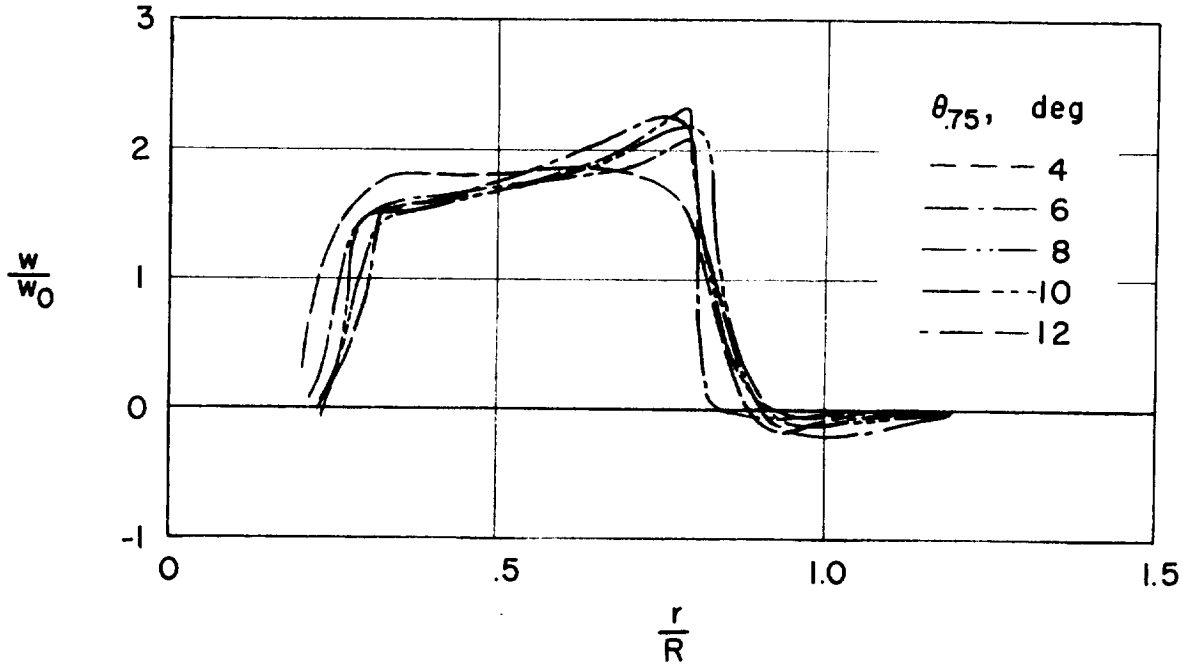

(d) ΩR = 1,000 fps.

Figure 3.- Continued.

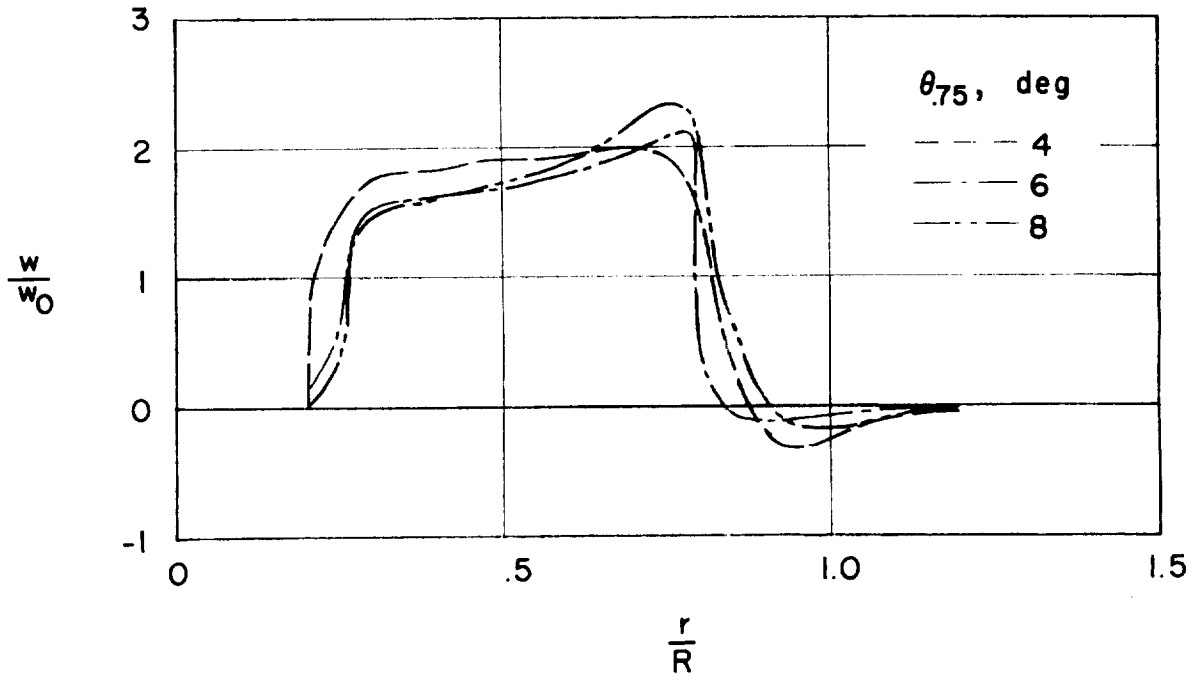

(e) ΩR = 1,100 fps.

Figure 3.- Concluded.

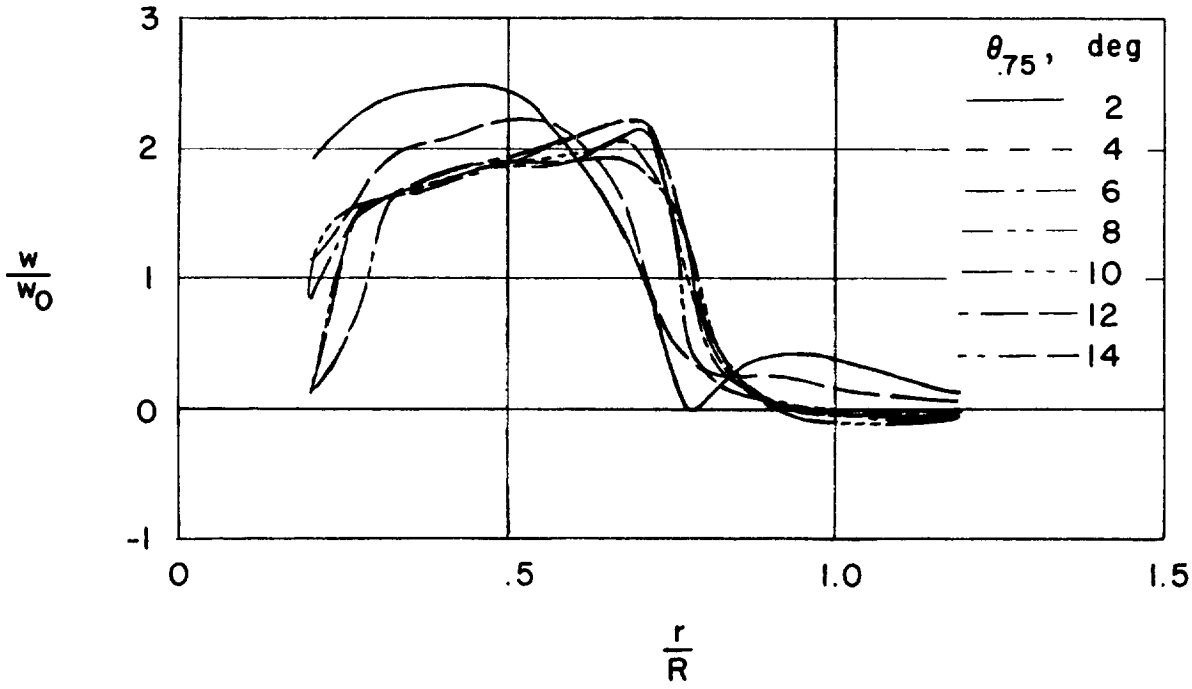

(a) ΩR = 500 fps.

Figure 4.- Effect of blade pitch angle at the 0.75R station on the induced velocities at $z/R = -0.45$.

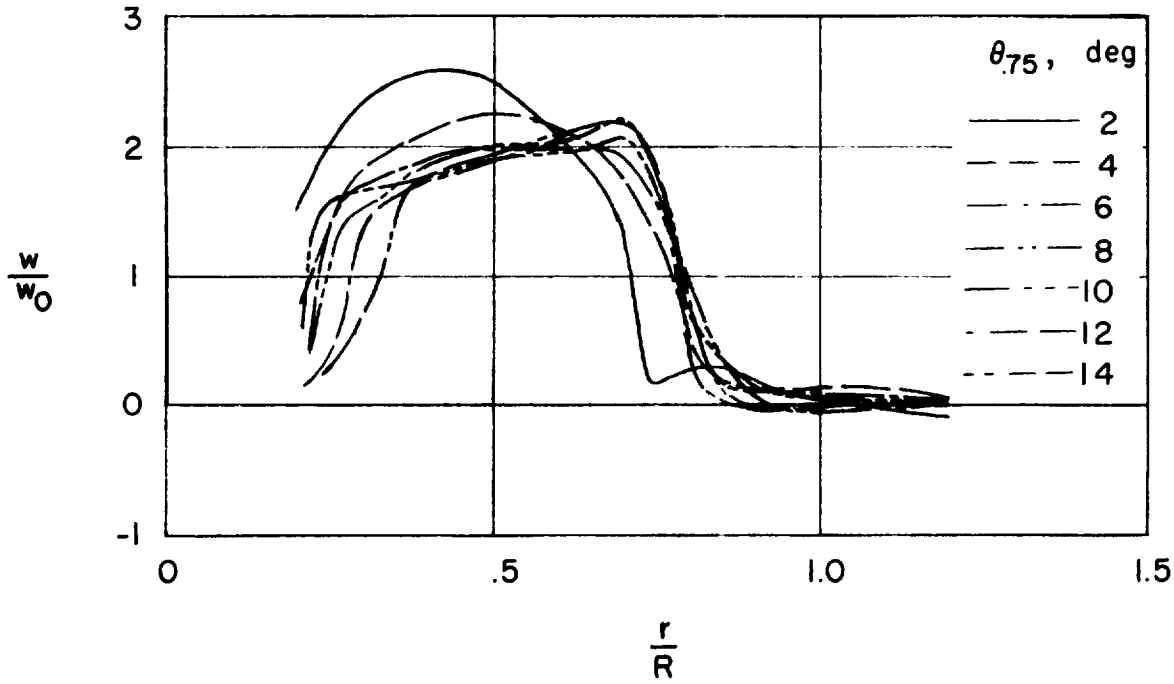

T-836

(b) ΩR = 700 fps.

Figure 4.- Continued.

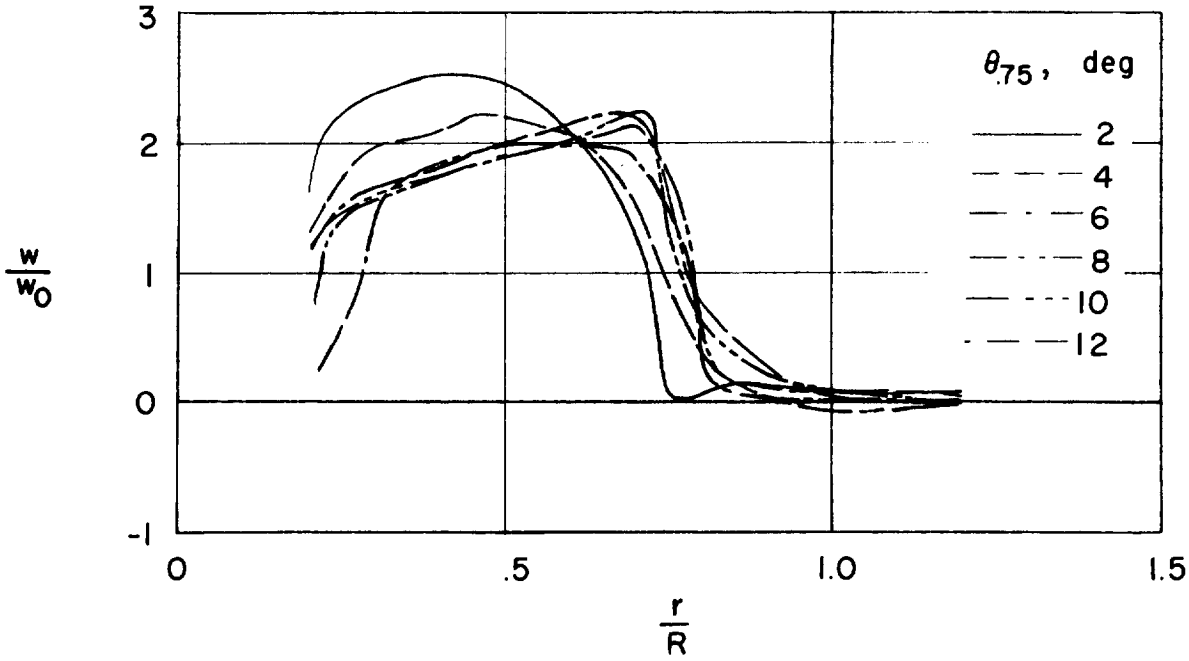

(c) ΩR = 900 fps.

Figure 4.- Continued.

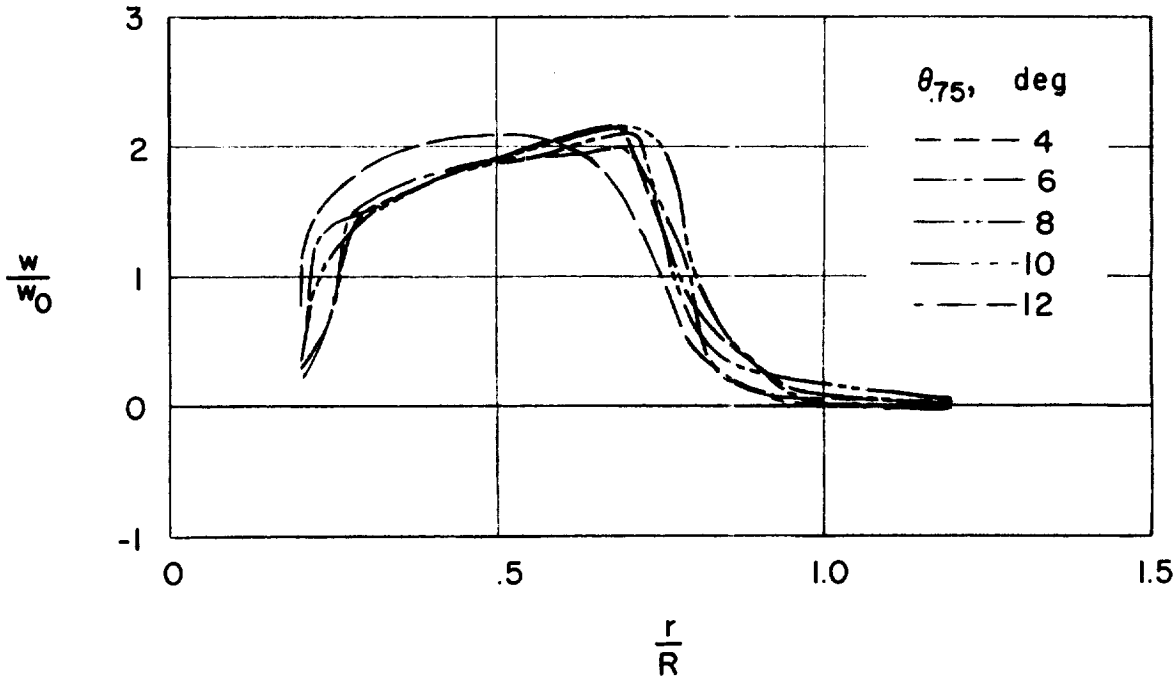

(d) ΩR = 1,000 fps.

Figure 4.- Continued.

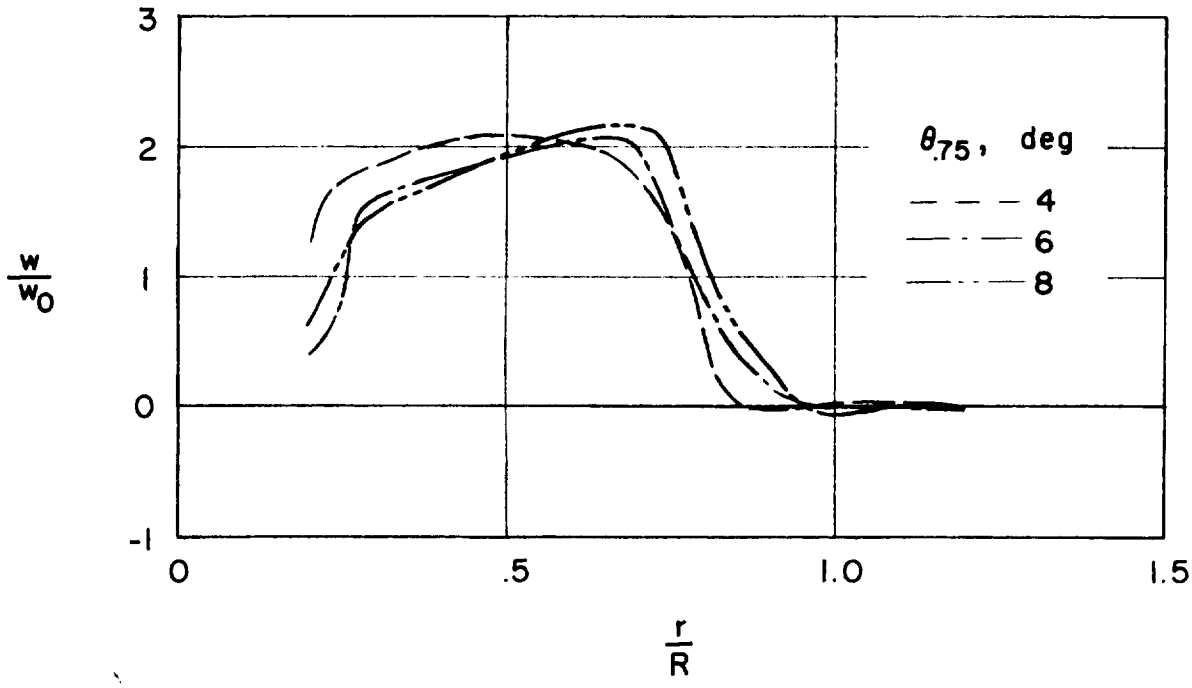

(e) ΩR = 1,100 fps.

Figure 4.- Concluded.

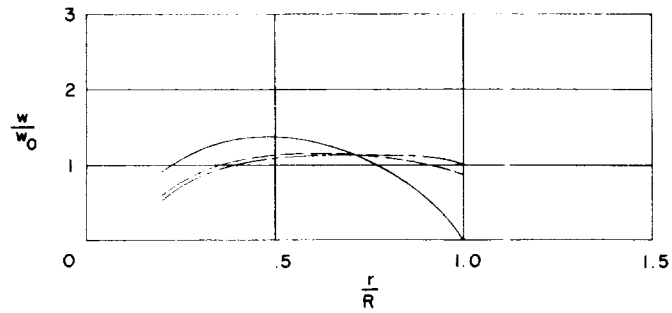

(a) Calculated, z/R = 0.

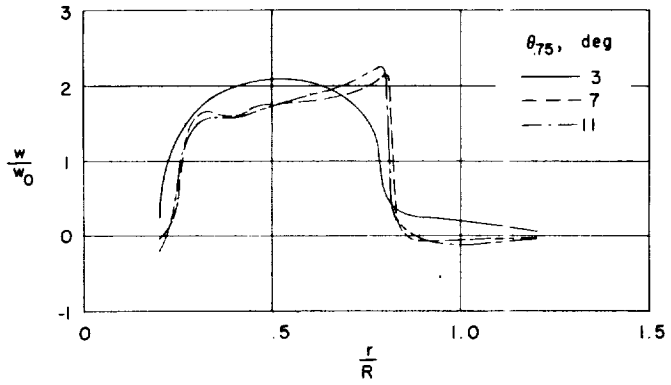

(b) Measured, z/R = -0.145.

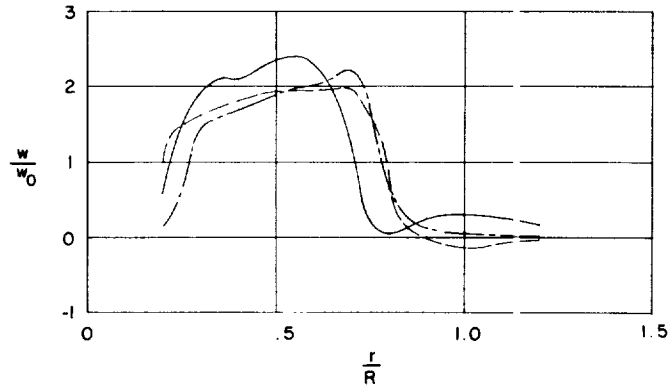

(c) Measured, z/R = -0.45.

Figure 5.- Comparison of calculated induced-velocity distribution in the plane of the rotor with the induced velocities measured in the wake. ΩR = 500 fps.

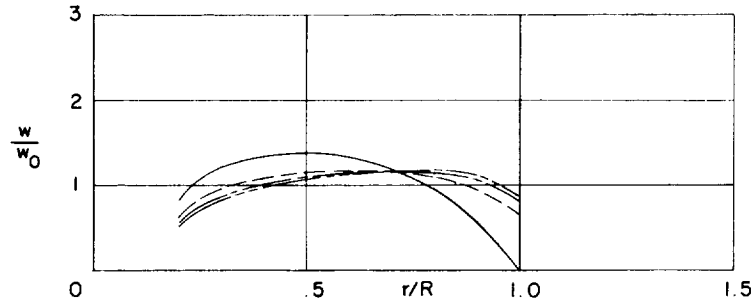

(a) Calculated, z/R = 0.

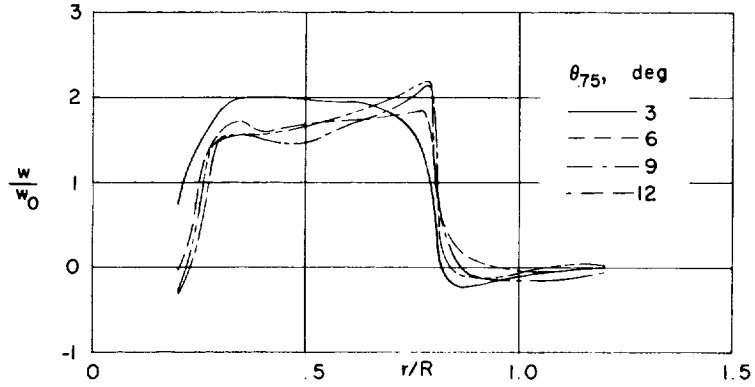

(b) Measured, z/R = -0.145.

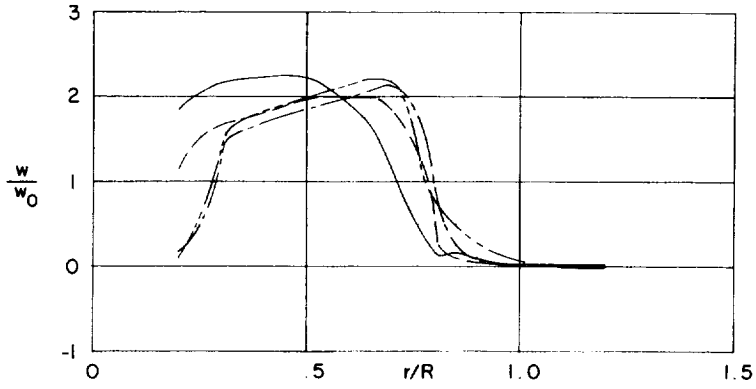

(c) Measured, z/R = -0.45.

Figure 6.- Comparison of calculated induced-velocity distribution in the plane of the rotor with the induced velocities measured in the wake. ΩR = 900 fps.

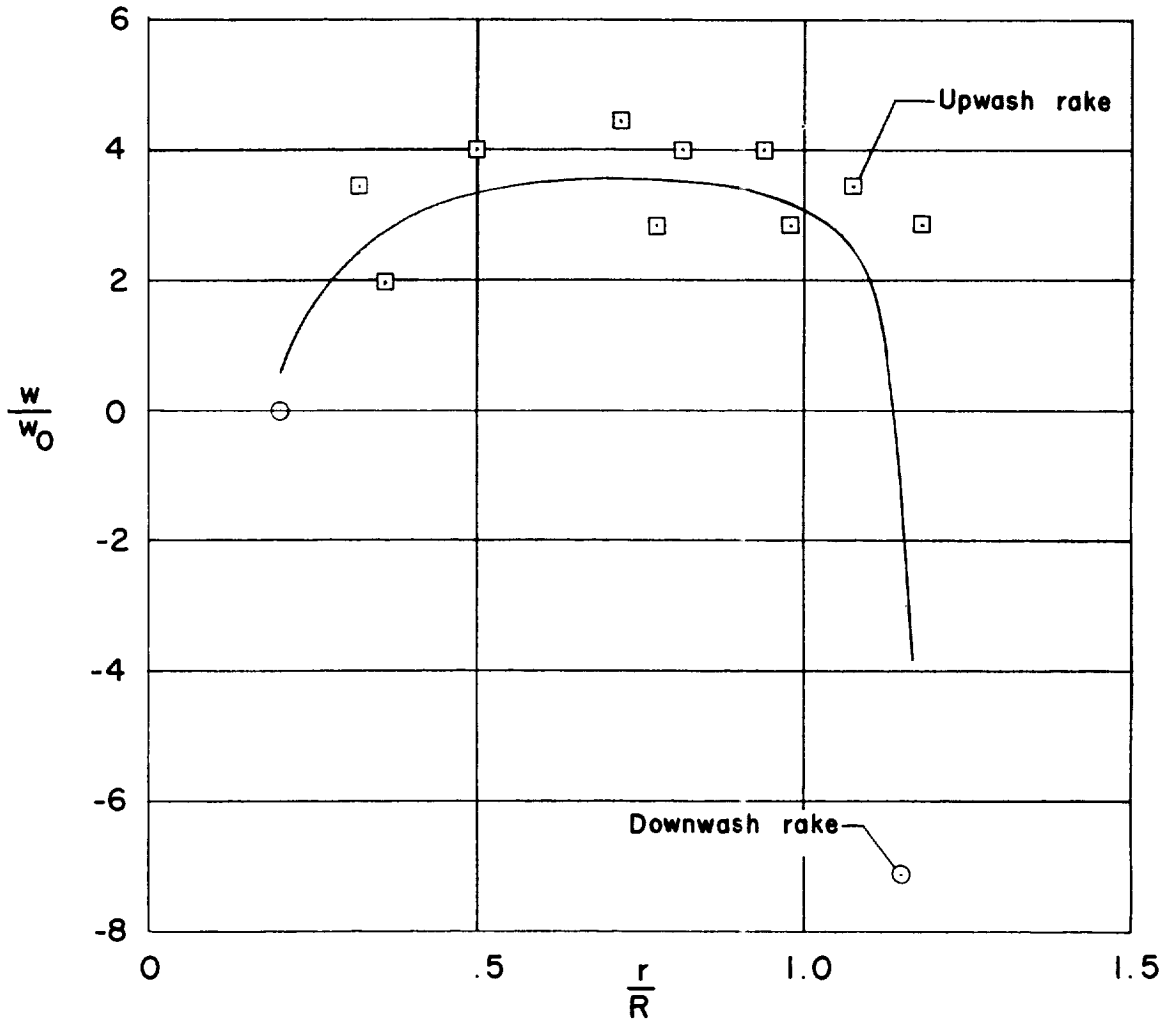

(a) z/R = -0.145.

Figure 7.- Induced-velocity distribution near zero lift. $\theta_{.75} = 0$; $w_o = +1.69$ fps.

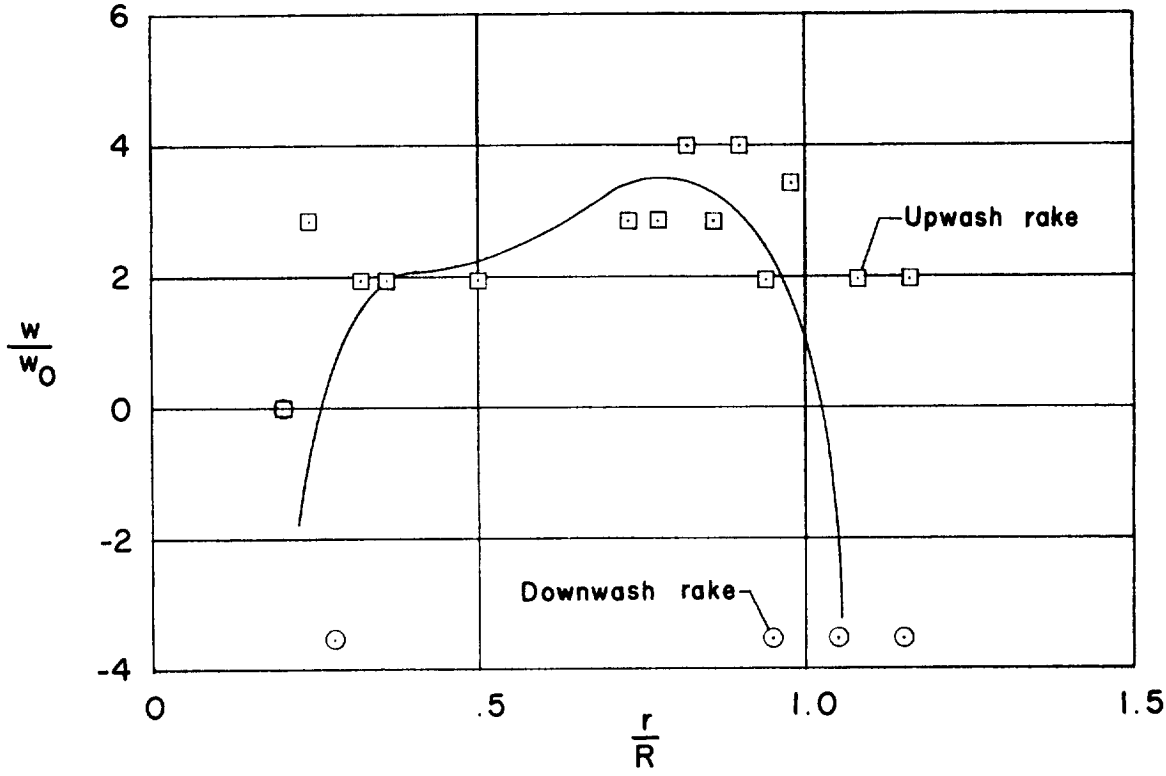

(b) z/R = -0.45.

Figure 7.- Concluded.

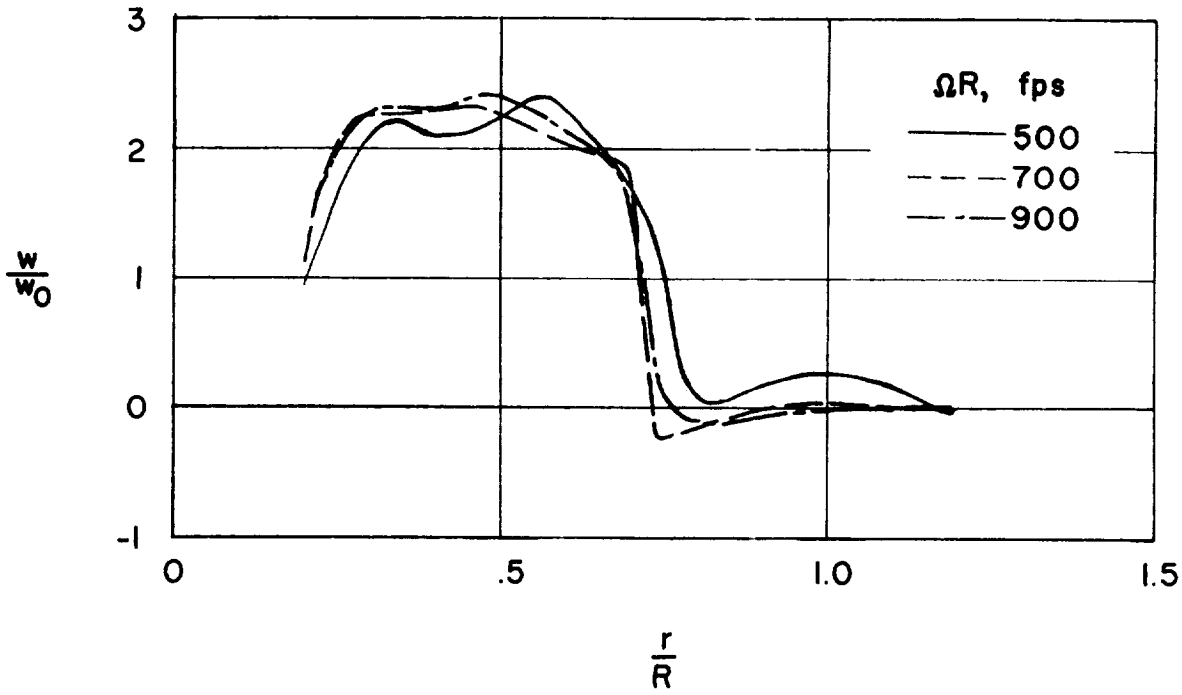

(a) $\theta_{.75} = 2^{\circ}$.

Figure 8.- Effect of tip speed on induced velocities in wake at $z/R = -0.145$.

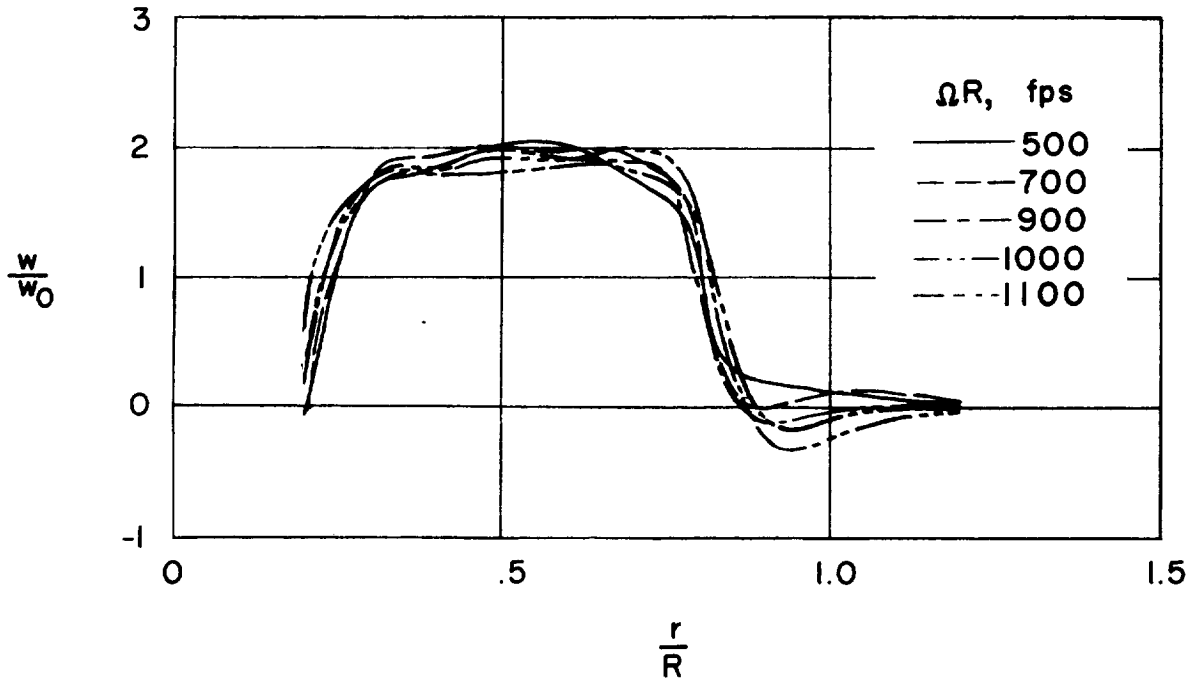

(b) $\theta_{.75} = 4^{\circ}$.

Figure 8.- Continued.

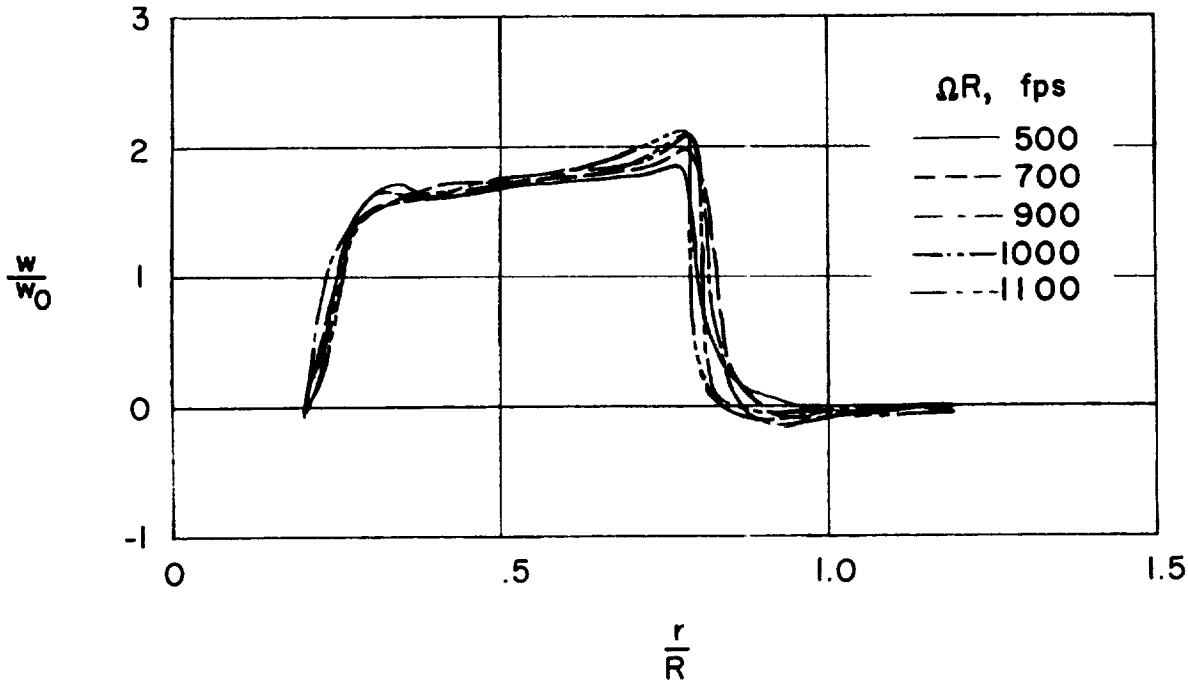

(c) $\theta_{.75} = 6^c$.

Figure 8.- Continued.

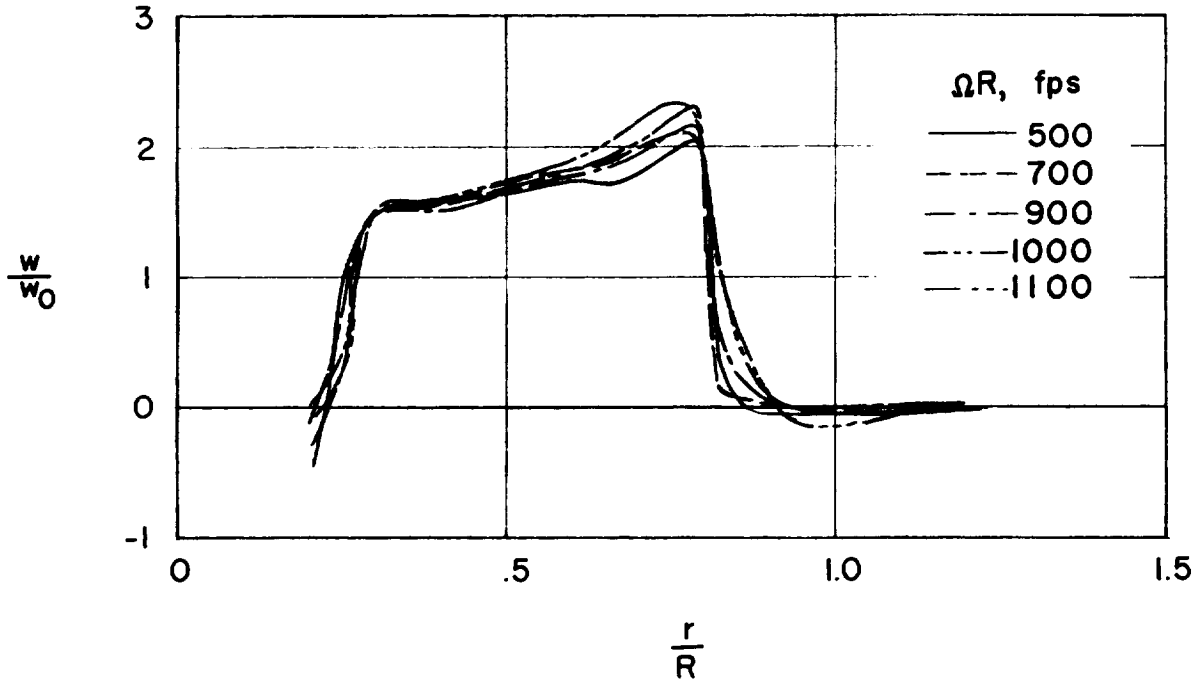

(d) $\theta_{.75} = 8^{\circ}$.

Figure 8.- Continued.

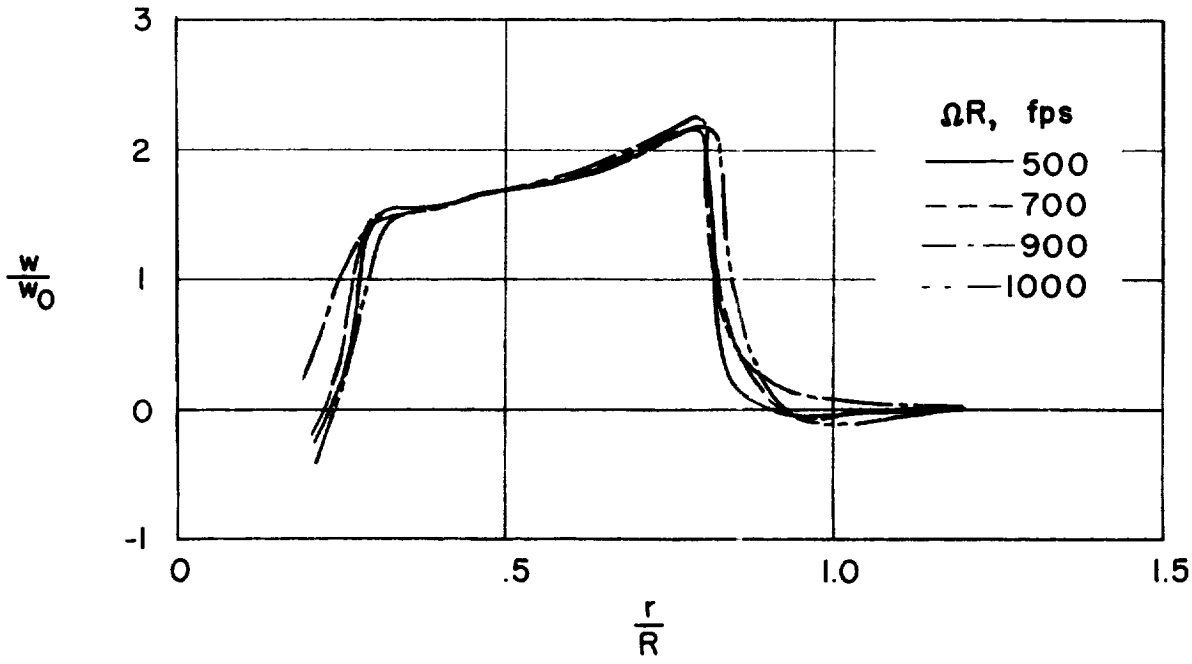

T.-836

(e) $\theta_{.75} = 10^{\circ}$.

Figure 8.- Continued.

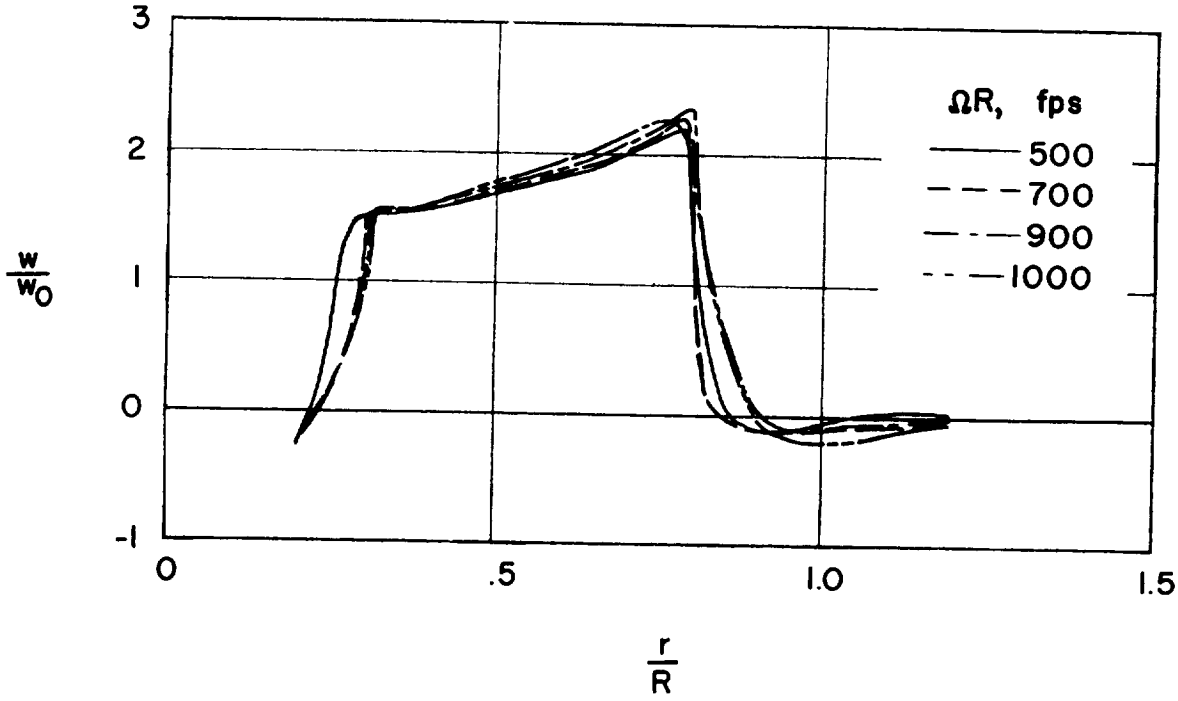

(f) $\theta_{.75} = 12^{\circ}$.

Figure 8.- Continued.

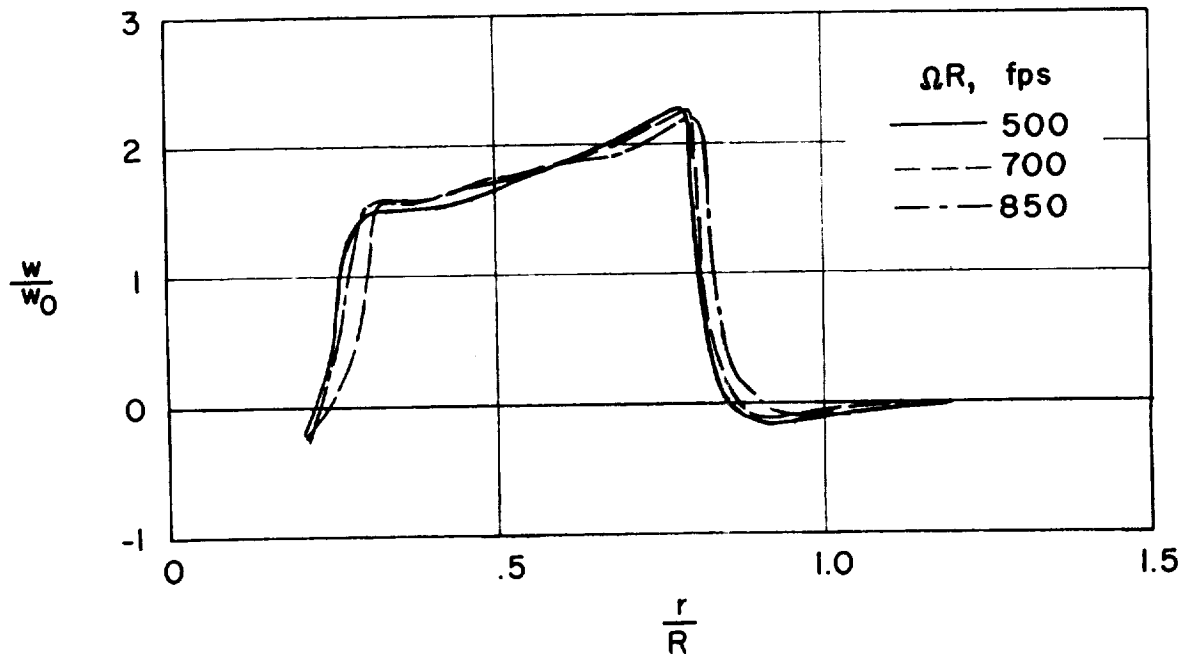

(g) $\theta_{.75} = 14^{\circ}$.

Figure 8.- Concluded.

L-836

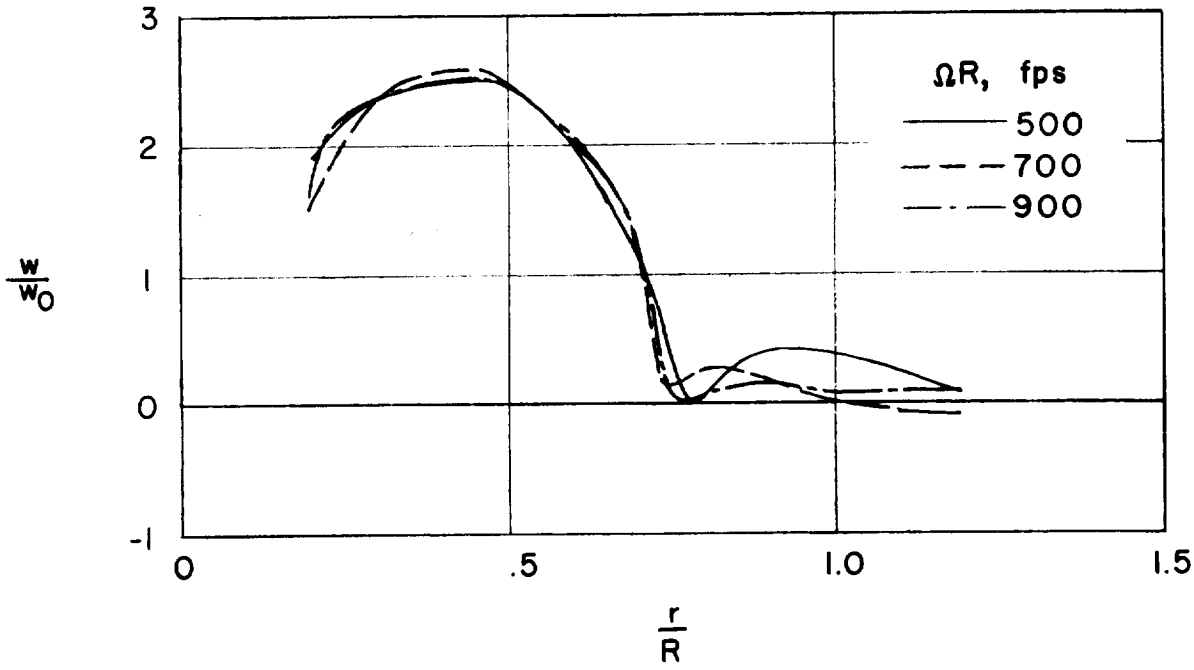

(a) $\theta_{.75} = 2^{\circ}$.

Figure 9.- Effect of tip speed on induced velocities in wake at $z/R = -0.45$.

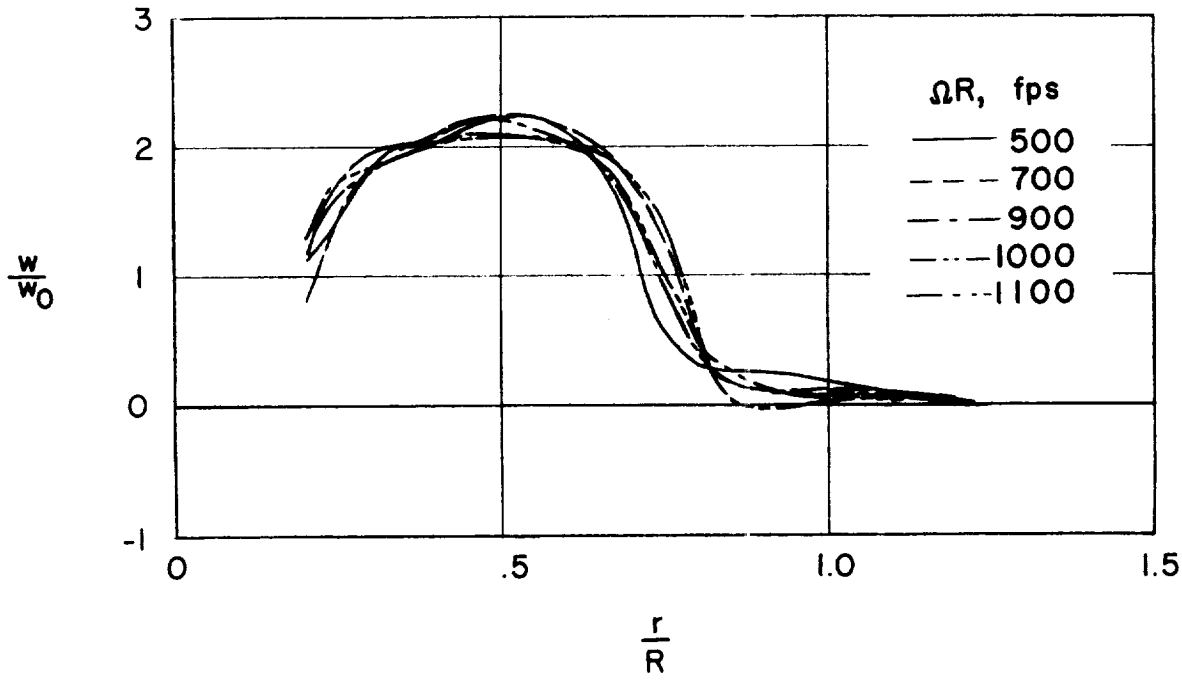

(b) $\theta_{.75} = 4^{\circ}$.

Figure 9.- Continued.

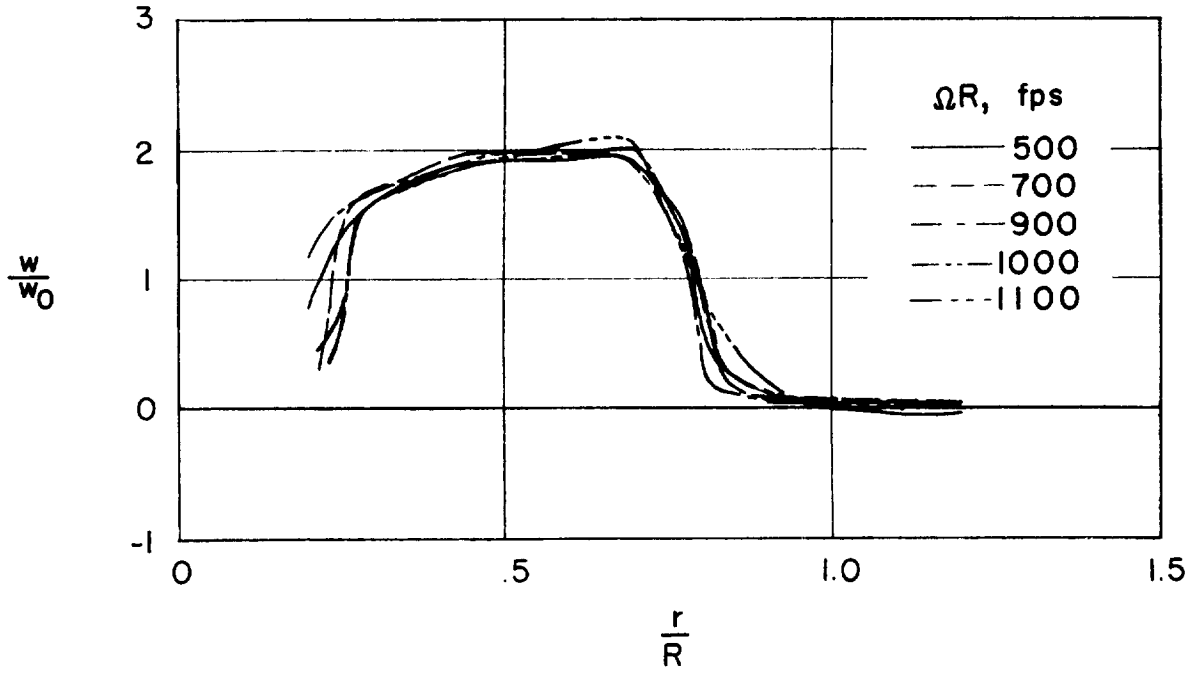

(c) $\theta_{.75} = 6^{\circ}$.

Figure 9.- Continued.

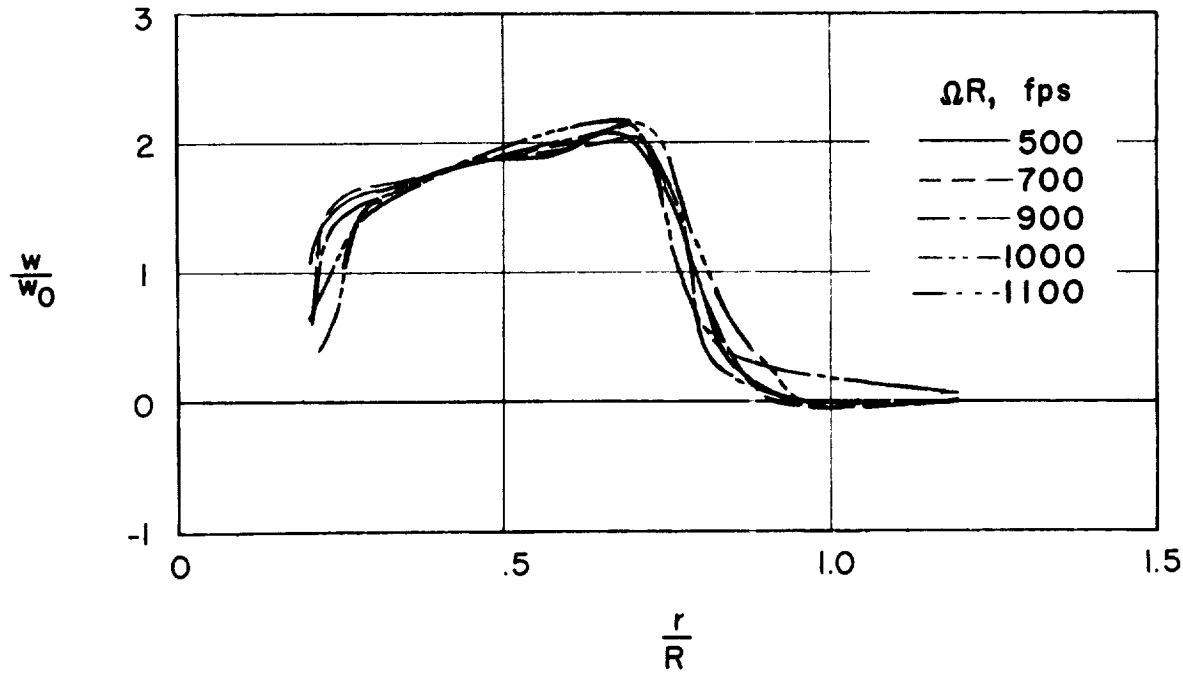

(d) $\theta_{.75} = 8^{\circ}$.

Figure 9.- Continued.

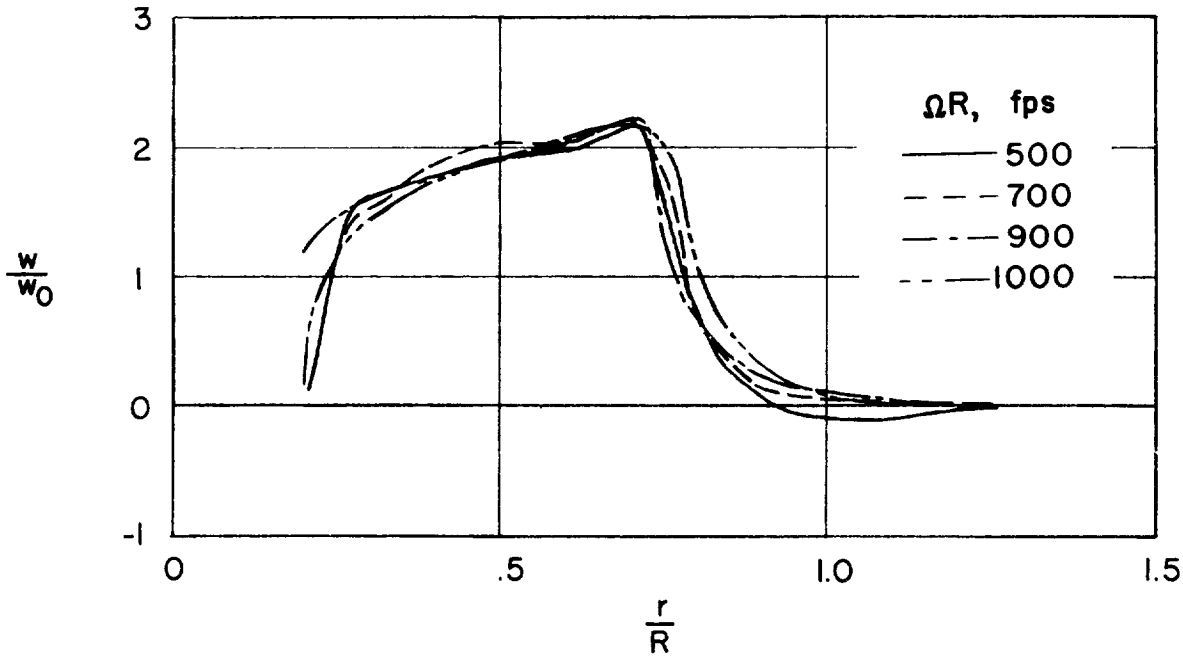

(e) $\theta_{.75} = 10^{\circ}$.

Figure 9.- Continued.

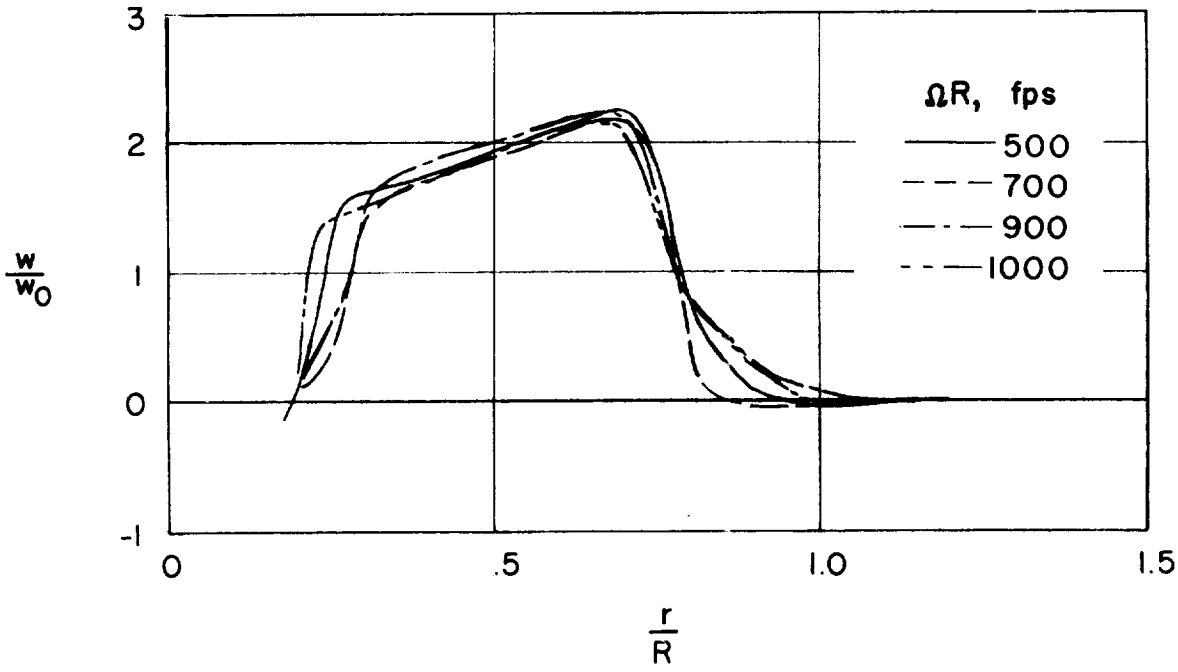

(f) $\theta_{.75} = 12^{\circ}$.

Figure 9.- Continued.

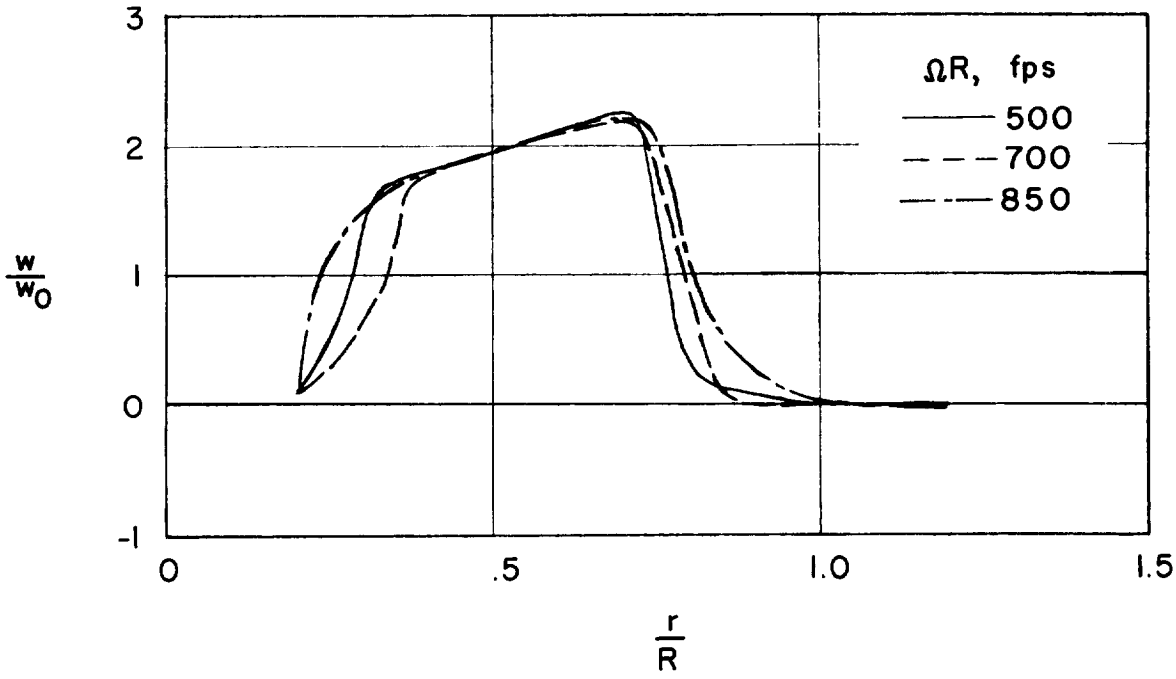

(g) $\theta_{.75} = 14^{\circ}$.

Figure 9.- Concluded.

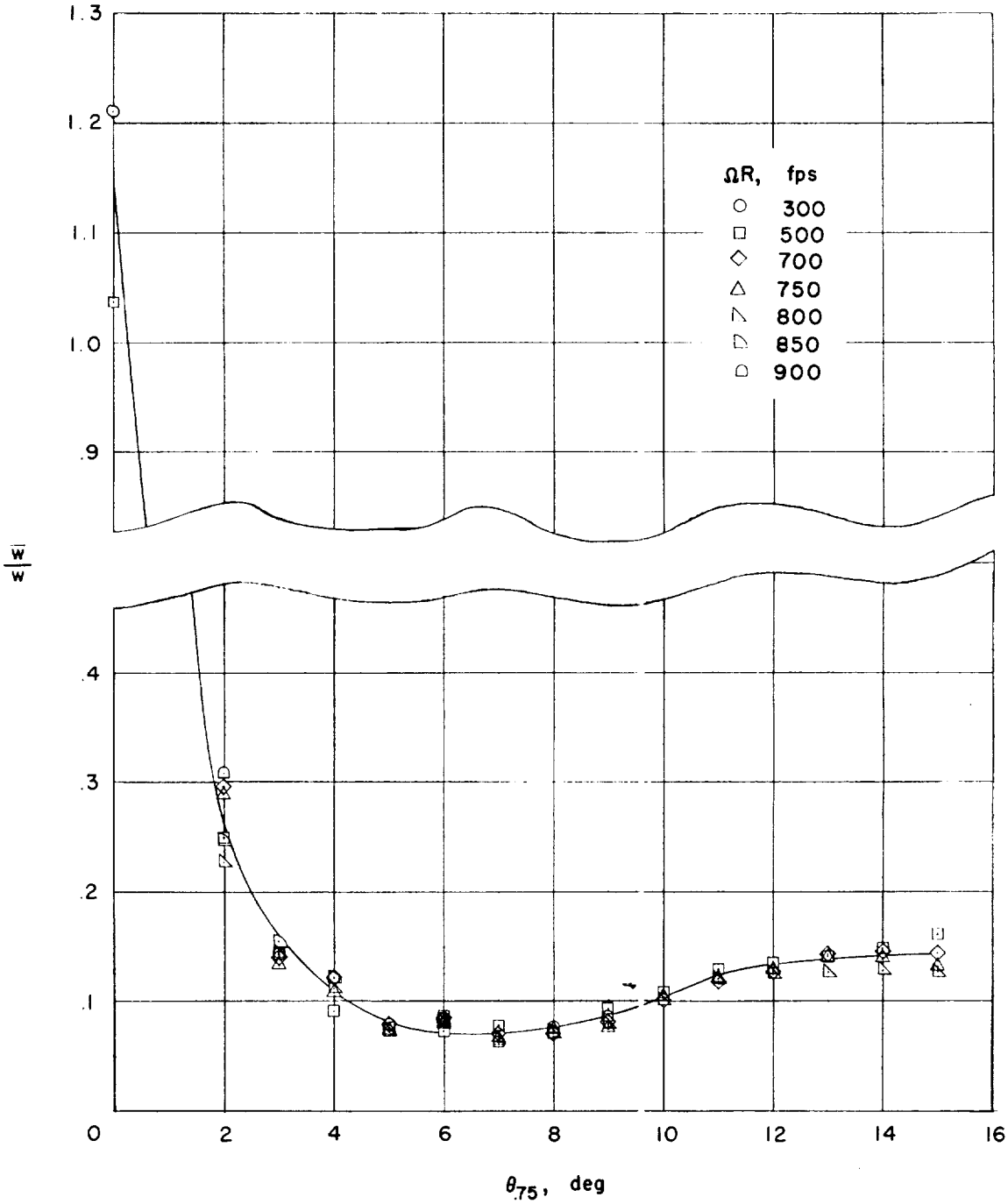

Figure 10.- Root-mean-square value of local fluctuating velocity, in terms of the local mean induced velocity, as a function of blade pitch angle. z/R = -0.145; r/R = 0.67.

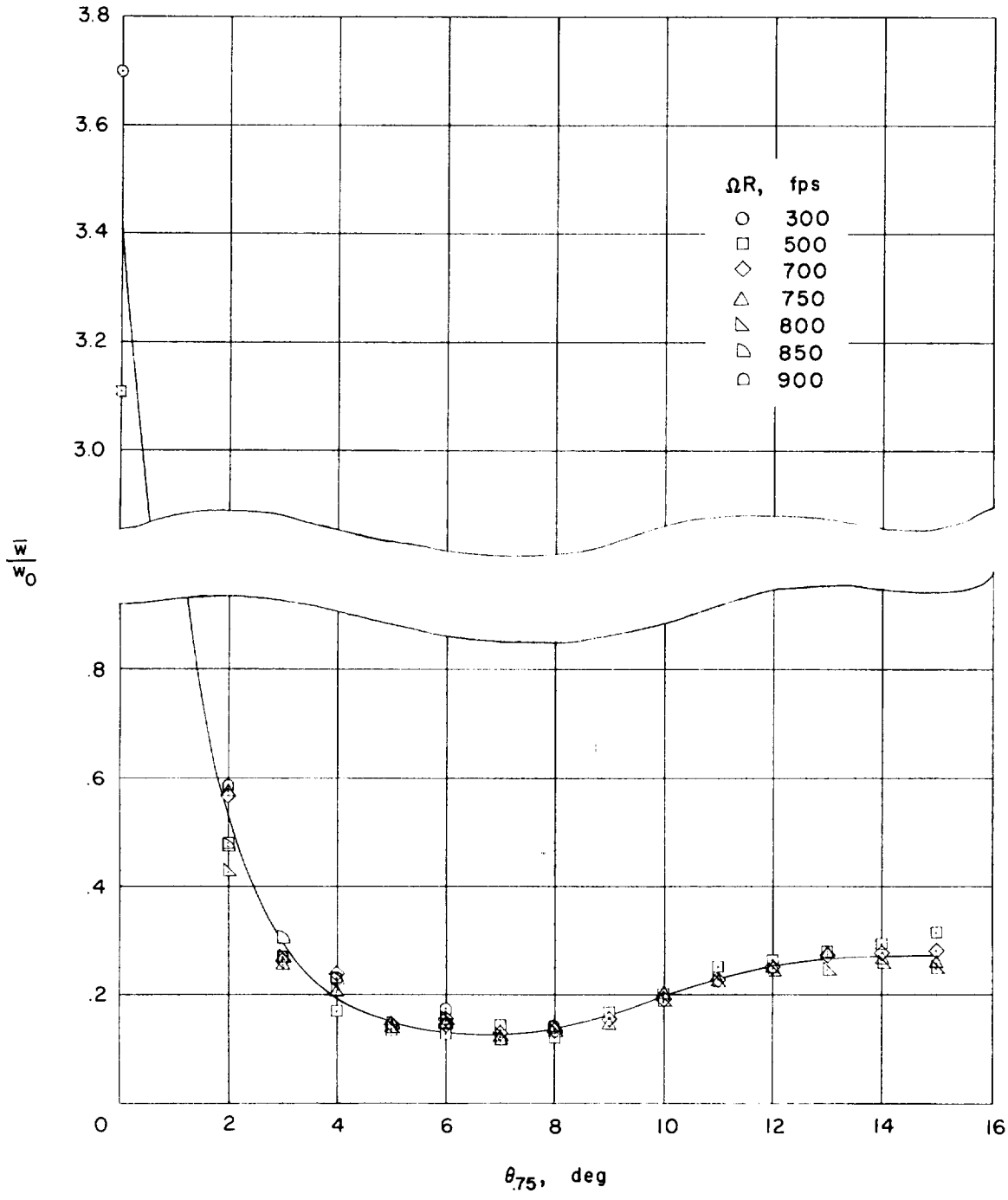

Figure 11.- Root-mean-square value of local fluctuating velocity, in terms of the average rotor induced velocity, as a function of blade pitch angle. z/R = -0.145; r/R = 0.67.

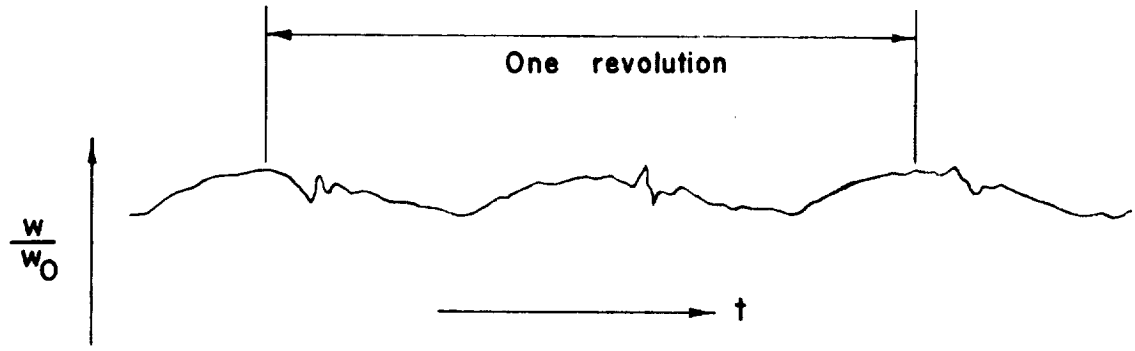

(a) Tip speed of 500 fps.

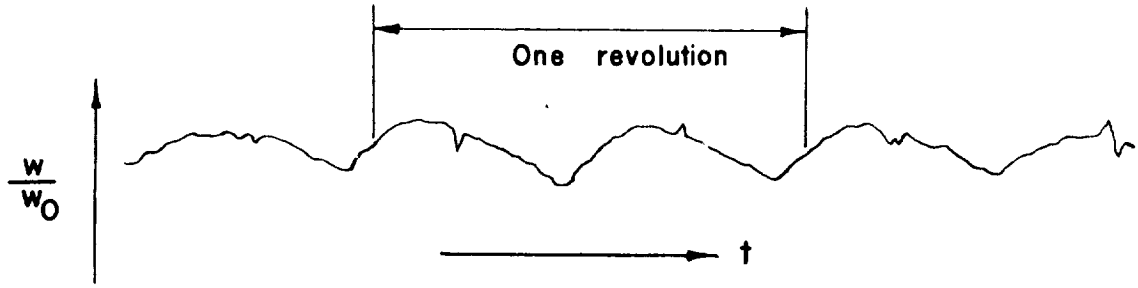

(b) Tip speed of 750 fps.

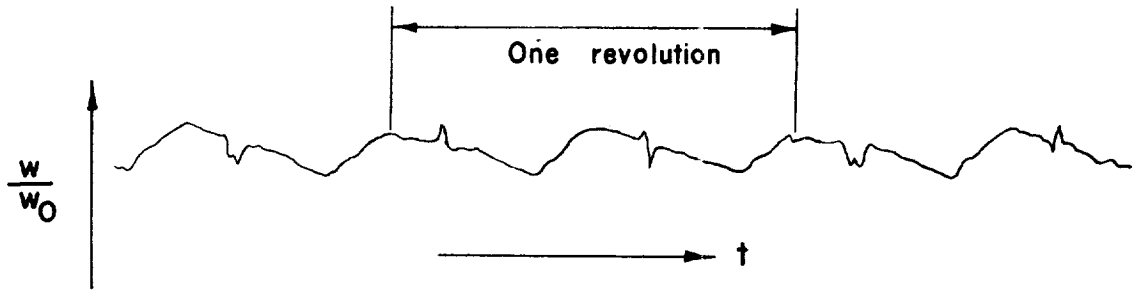

(c) Tip speed of 800 fps.

Figure 12.- Time history of normalized velocities in wake as measured with hot-wire anemometer. $\theta_{.75} = 10^{\circ}$; $z/R = -0.145$; $r/R = 0.67$.

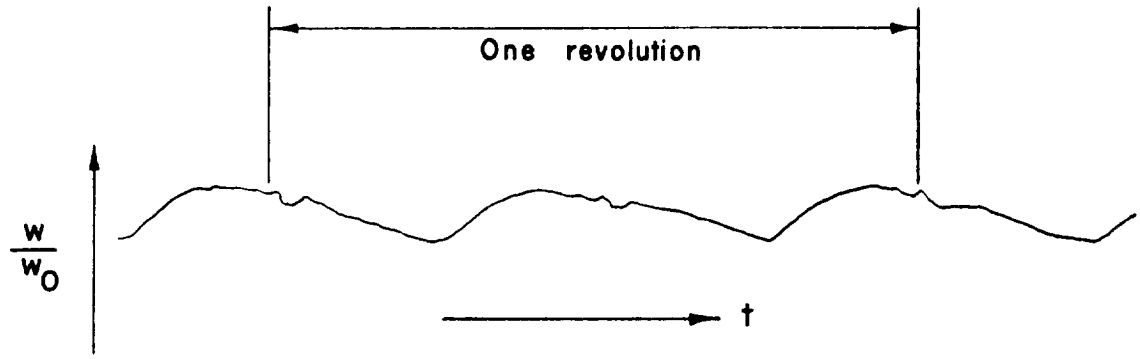

(a) Tip speed of 500 fps.

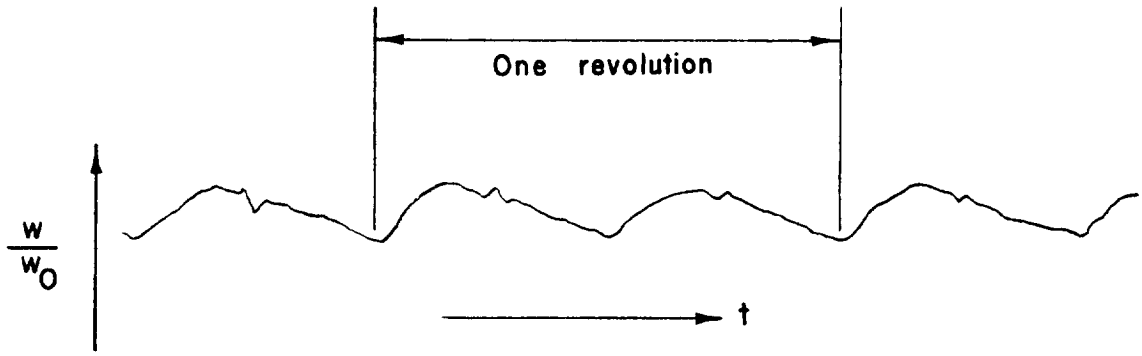

(b) Tip speed of 700 fps.

Figure 13.- Time history of normalized velocities in wake as measured with hot-wire anemometer. $\theta_{.75} = 12^{\circ}$; $z/R = -0.145$; $r/R = 0.67$.

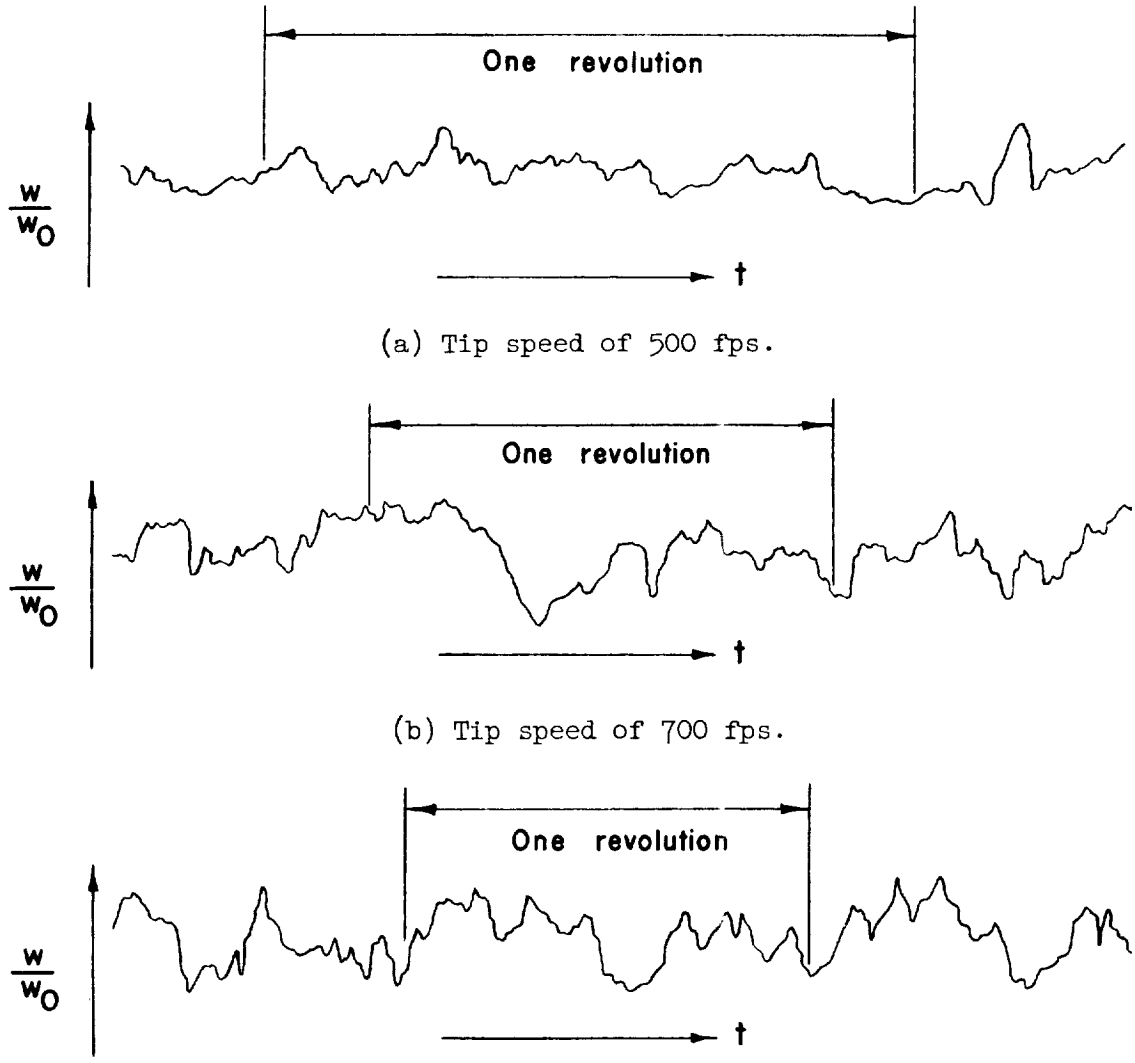

(a) Tip speed of 500 fps.

(b) Tip speed of 700 fps.

(c) Tip speed of 800 fps.

Figure 14.- Time history of normalized velocities in wake as measured with hot-wire anemometer. (Velocity scale compressed by factor of 10 as compared with figs. 12 and 13.) $\theta_{.75} = 2^{\circ}$; $z/R = -0.145$; $r/R = 0.67$.

L-836